Supporting information for

Recycling primary lithium batteries using a coordination chemistry approach: recovery of lithium and manganese residues in the form of industrially important materials

Rafał Petrus,[a,*] Adrian Kowaliński,[a] Tadeusz Lis[b]

[a]Faculty of Chemistry, Wrocław University of Science and Technology, 23 Smoluchowskiego, 50-370 Wrocław, Poland

[b]Faculty of Chemistry, University of Wrocław, 14 F. Joliot-Curie, 50-383 Wrocław, Poland

Corresponding author:

Dr. Rafał Petrus, D.Sc., rafal.petrus@pwr.edu.pl

Contents

Crystallographic Data for Compounds 1 - 9.

Table S1. Crystal and data collection parameters for compounds **1 - 9**.

Crystal	**1_m**	**1_o**	**2**	**3**
Chemical formula	$C_{10}H_{15}LiO_5$	$C_{10}H_{15}LiO_5$	$C_{16}H_{15}LiO_6$	$C_{20}H_{26}Li_2O_8$
Formula Mass	222.16	222.16	310.22	408.29
Crystal system	Monoclinic	Orthorhombic	Monoclinic	Monoclinic
Space group	$C2/c$	$Pna2_1$	$P2_1$/c	$C2$/c
a/Å	19.757 (8)	16.660 (6)	4.978 (10)	23.405 (4)
b/Å	6.8303 (15)	10.120 (2)	11.479 (2)	8.959 (12)
c/Å	18.858 (9)	7.004 (17)	26.144 (5)	20.406 (3)
α/°				
β/°	115.43 (5)		94.95 (2)	94.63(2)
γ/°				
Unit cell volume/Å^3	2298.2 (18)	1180.9 (6)	1488.4 (5)	4264.8 (11)
Temperature/K	100	100	100	100
Z	8	4	4	8
Radiation type	MoKα	MoKα	CuKα	MoKα
Absorption coefficient, μ/mm^{-1}	0.101	0.098	0.881	0.096
No. of reflections measured	5504	12820	34153	20355
No. of independent reflections	2500	2557	2804	4647
No. of observed ($I > 2\sigma(I)$) reflections	2194	2473	2351	4475
R_{int}	0.0151	0.0165	0.0548	0.0468
Final R_1 values ($I > 2\sigma(I)$)	0.0387	0.0245	0.0467	0.0773
Final $wR(F^2)$ values ($I > 2\sigma(I)$)	0.0991	0.0667	0.1224	0.1967
Final R_1 values (all data)	0.0452	0.0256	0.0549	0.0787
Final $wR(F^2)$ values (all data)	0.1040	0.0673	0.1292	0.1972
Goodness of fit on F^2	1.049	1.061	1.070	1.210
Δρmax/eÅ^{-3}	0.340	0.200	0.318	0.365
Δρmin/eÅ^{-3}	-0.270	-0.153	-0.370	-0.351

Crystal	**4_m**	**4_t**	**4a**	**5**
Chemical formula	$C_{16}H_{18}Li_2O_8$	$C_{16}H_{18}Li_2O_8$	$C_{16.80}H_{19.60}Li_2O_8$	$C_{46}H_{60}Li_4O_{20}$
Formula Mass	352.18	352.18	363.40	960.70
Crystal system	Monoclinic	Triclinic	Monoclinic	Triclinic
Space group	$P2_1/n$	$P\bar{1}$ $\bar{1}$	$C2/c$	$P\bar{1}$ $\bar{1}$
a/Å	6.431 (16)	6.442 (3)	26.154 (5)	10.112 (2)
b/Å	10.351(2)	10.346 (2)	10.384 (18)	11.581 (3)
c/Å	24.580(6)	12.498 (2)	6.473 (11)	11.920 (3)
α/°		99.32 (2)		76.17 (2)
β/°	90.61 (3)	91.04 (2)	102.25 (3)	85.10 (2)
γ/°		90.12 (2)		65.65 (3)
Unit cell volume/Å^3	1636.1 (7)	821.8 (4)	1717.9 (6)	1234.7 (6)
Temperature/K	100	100	100	100
Z	4	2	4	1
Radiation type	CuKα	CuKα	CuKα	MoKα
Absorption coefficient, μ/mm^{-1}	0.952	0.948	0.924	0.099
No. of reflections measured	11081	5688	7773	22577
No. of independent reflections	2896	2994	1650	5956
No. of observed ($I > 2\sigma(I)$) reflections	2624	2195	1540	5366
R_{int}	0.0375	0.0710	0.0230	0.0156
Final R_1 values ($I > 2\sigma(I)$)	0.0672	0.1079	0.0373	0.0313
Final $wR(F^2)$ values ($I > 2\sigma(I)$)	0.1856	0.2720	0.0990	0.0825
Final R_1 values (all data)	0.0710	0.1235	0.0394	0.0347
Final $wR(F^2)$ values (all data)	0.1916	0.3029	0.1005	0.0842
Goodness of fit on F^2	1.063	1.100	1.079	1.065
Δρmax/eÅ^{-3}	0.686	0.987	0.292	0.355
Δρmin/eÅ^{-3}	-0.334	-0.550	-0.469	-0.189

Crystal	**7**	**7a**	**9**
Chemical formula	$C_{54}H_{54}Li_6O_{18}$	$C_{51}H_{48}Li_6O_{18}$	$C_{57.24}H_{64.48}Li_6O_{23.62}$
Formula Mass	1032.61	990.53	1172.00
Crystal system	Triclinic	Triclinic	Triclinic
Space group	$P\bar{1}$ $\bar{1}$	$P\bar{1}$ $\bar{1}$	$P\bar{1}$
a/Å	8.377 (2)	8.285 (2)	10.823 (3)
b/Å	12.233 (3)	12.146 (4)	12.501 (3)
c/Å	13.360 (3)	13.254 (4)	13.588 (4)
α/°	68.71 (3)	67.26 (3)	102.57 (2)
β/°	80.75 (3)	78.53 (2)	108.41 (2)
γ/°	89.55 (3)	87.65 (2)	111.69 (2)
Unit cell volume/Å^3	1257.2 (6)	1204.6 (7)	1499.8 (8)
Temperature/K	100	100	100
Z	1	1	1
Radiation type	MoKα	MoKα	MoKα
Absorption coefficient, μ/mm^{-1}	0.100	0.101	0.099
No. of reflections measured	9334	9615	11032
No. of independent reflections	5460	5160	6274
No. of observed ($I > 2\sigma(I)$) reflections	4533	4306	4071
R_{int}	0.0204	0.0155	0.0387
Final R_1 values ($I > 2\sigma(I)$)	0.0370	0.0392	0.0739
Final $wR(F^2)$ values ($I > 2\sigma(I)$)	0.0867	0.0907	0.1851
Final R_1 values (all data)	0.0488	0.0509	0.1100
Final $wR(F^2)$ values (all data)	0.0942	0.0970	0.2227
Goodness of fit on F^2	1.028	1.050	1.051
Δρmax/eÅ^{-3}	0.284	0.283	0.406
Δρmin/eÅ^{-3}	-0.224	-0.215	-0.322

Table S2. Continuous-shape measurements (CShM) of the coordination environment around Li in **1-9**.

compound	atom	donor atoms	polyhedron	*S* parameter
1$_{orthorhombic}$	Li1	O_4	tetrahedron	0.774
1$_{monoclinic}$	Li1	O_4	tetrahedron	0.945
2	Li1	O_4	tetrahedron	3.116
3	Li1	O_4	tetrahedron	2.616
	Li2	O_4	tetrahedron	2.520
4$_{monoclinic}$	Li1	O_4	tetrahedron	1.293
	Li2	O_4	tetrahedron	1.216
4$_{triclinic}$	Li1	O_4	tetrahedron	1.260
	Li2	O_4	tetrahedron	1.256
4a	Li1	O_4	tetrahedron	1.261
5	Li1	O_4	tetrahedron	1.349
	Li2	O_4	tetrahedron	1.539
6	Li1	O_4	axially vacant trigonal bipyramid	2.431
	Li2	O_4	tetrahedron	2.444
	Li3	O_4	axially vacant trigonal bipyramid	2.326
7	Li1	O_4	tetrahedron	2.498
	Li2	O_4	tetrahedron	2.341
	Li3	O_4	tetrahedron	2.553
7a	Li1	O_4	tetrahedron	2.570
	Li2	O_4	tetrahedron	2.497
	Li3	O_4	tetrahedron	2.366
9	Li1	O_4	tetrahedron	1.766
	Li2	O_4	tetrahedron	1.085
	Li3	O_4	tetrahedron	1.511

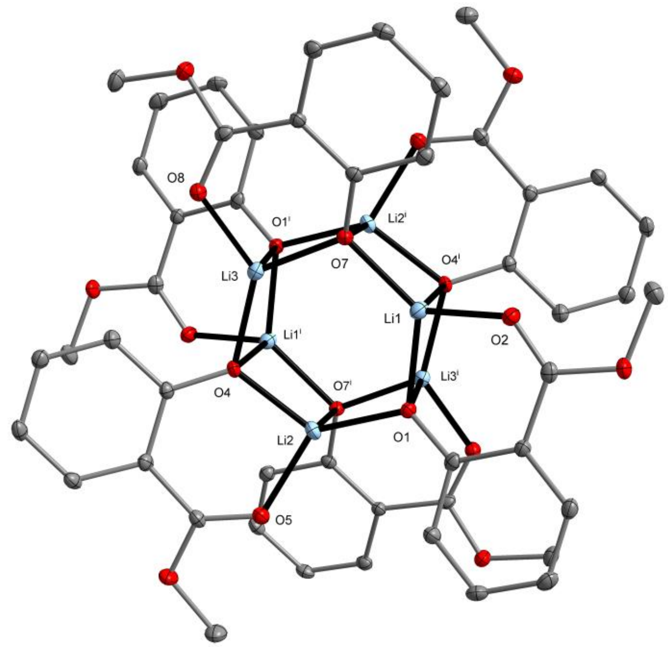

Figure S1. Molecular structure of $[Li_6(OAr)_6]$ (**6**) for ArOH = methyl salicylate. Displacement ellipsoids are drawn at the 25% probability level. The hydrogen atoms of the alkyl groups are omitted for clarity [symmetry code: (i) $-x+1$, $-y+1$, $-z+1$]. Reproduced by permission of The Royal Society of Chemistry.[1]

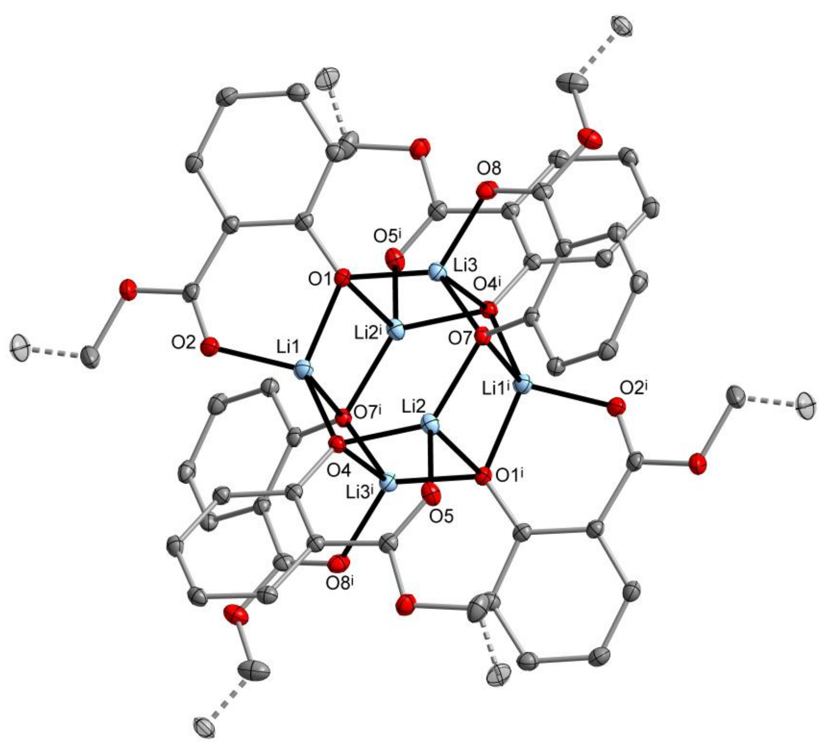

Figure S2. Molecular structure of $[Li_6(OAr)_6]$ (**7a**), for ArOH = methyl salicylate (0.5), ethyl salicylate (0.5). Displacement ellipsoids are drawn at the 25% probability level. The hydrogen atoms of the alkyl groups are omitted for clarity [symmetry code: (i) $-x+1$, $-y+1$, $-z+1$].

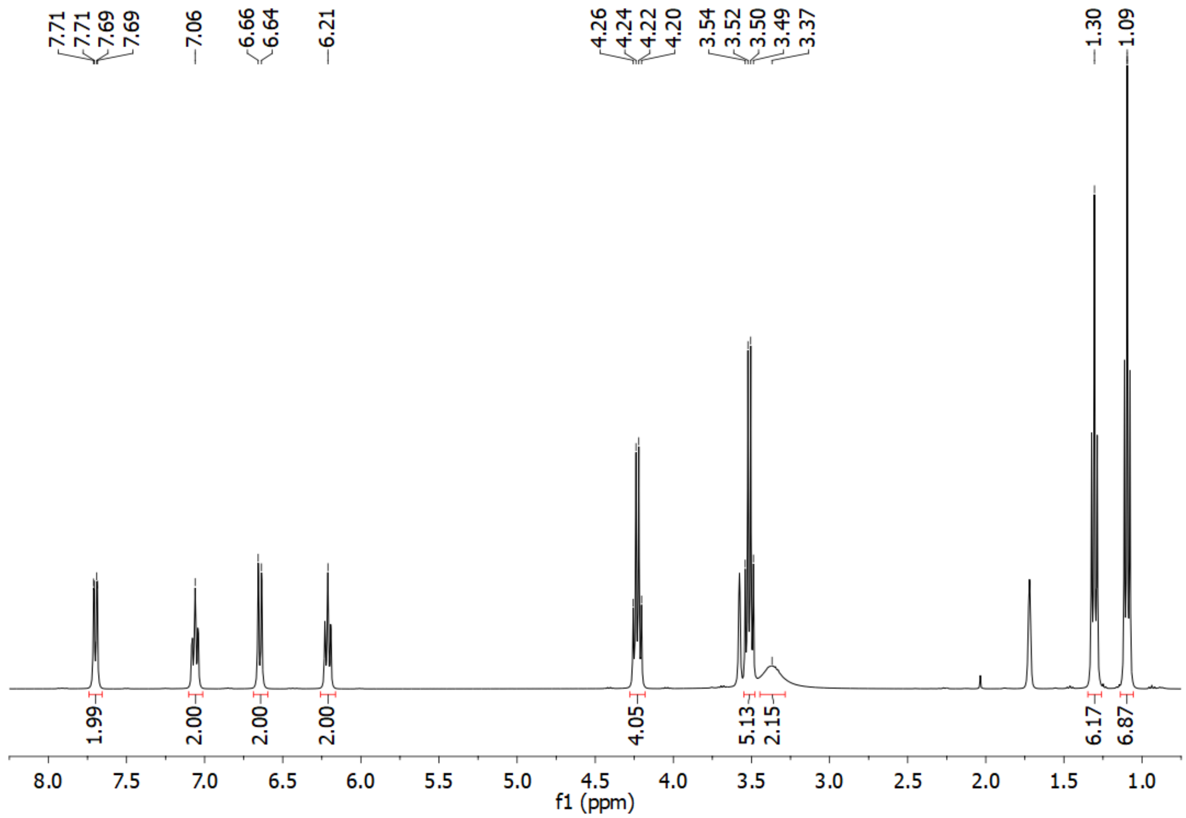

Figure S3. ^{1}H NMR spectrum of **3**.

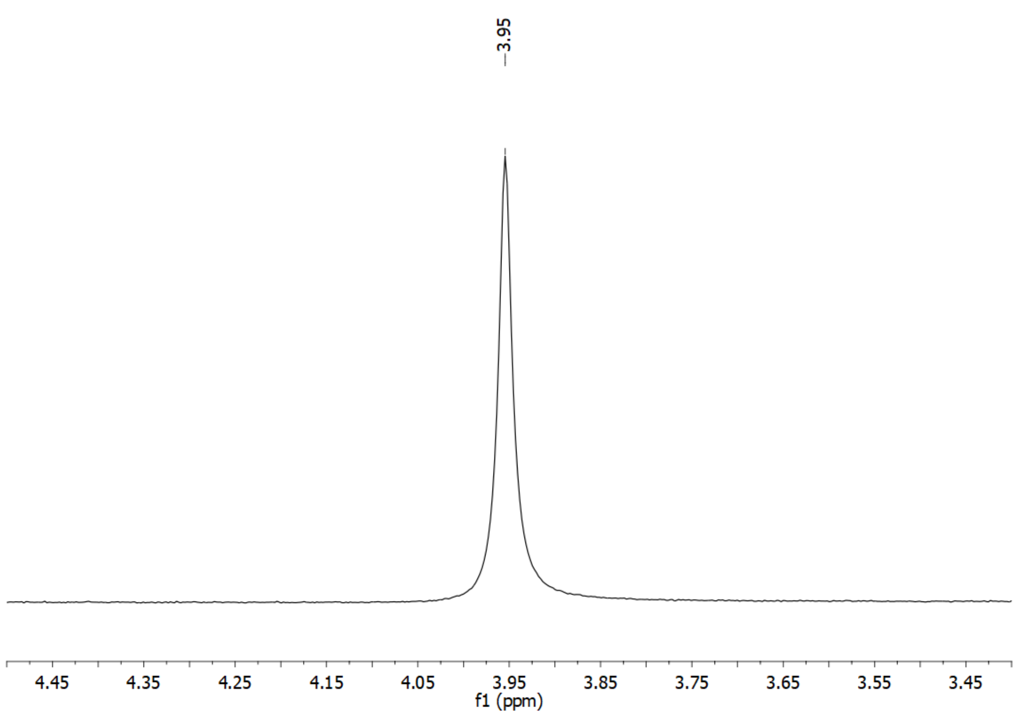

Figure S4. ^{7}Li NMR spectrum of **3**.

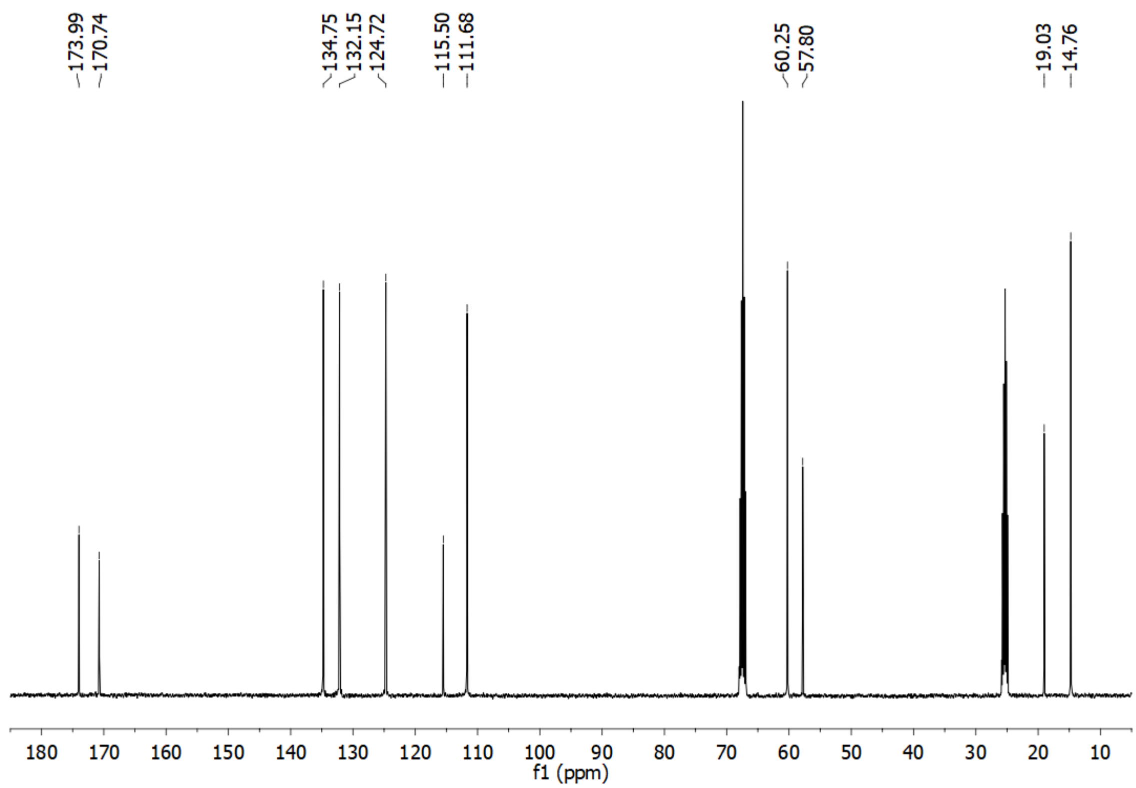

Figure S5. ^{13}C NMR spectrum of **3**.

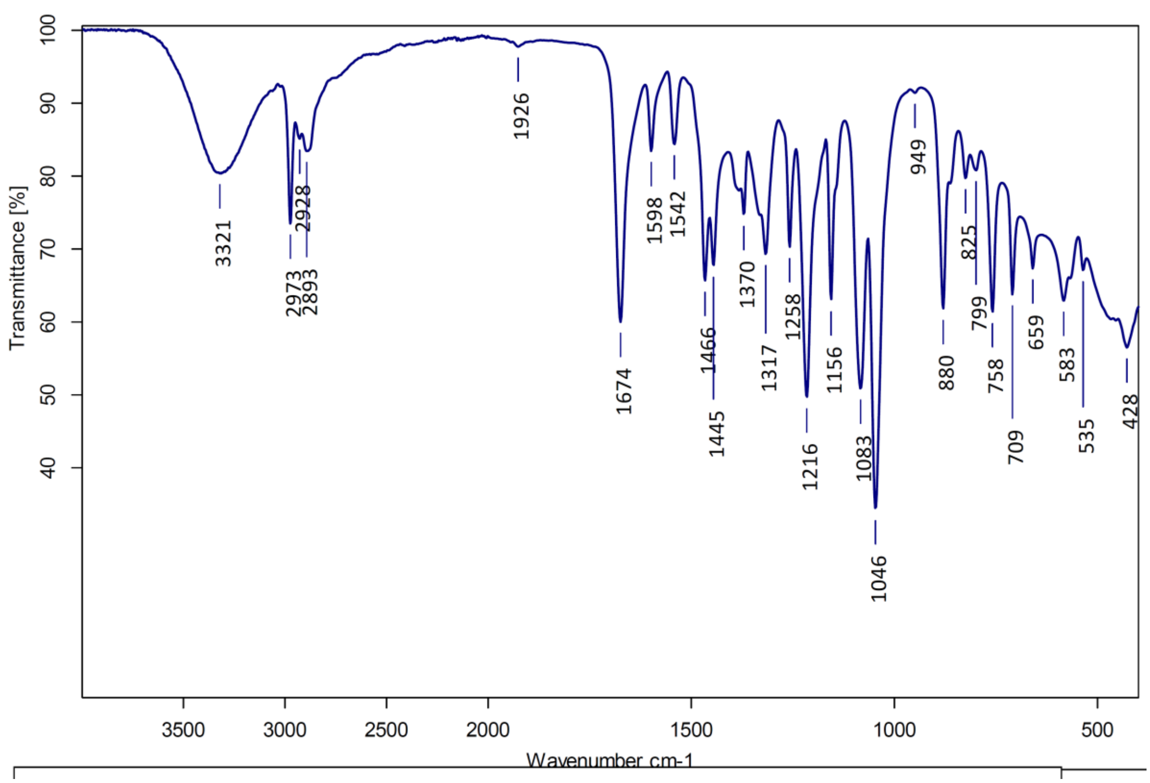

Figure S6. FTIR-ATR spectrum of **3**.

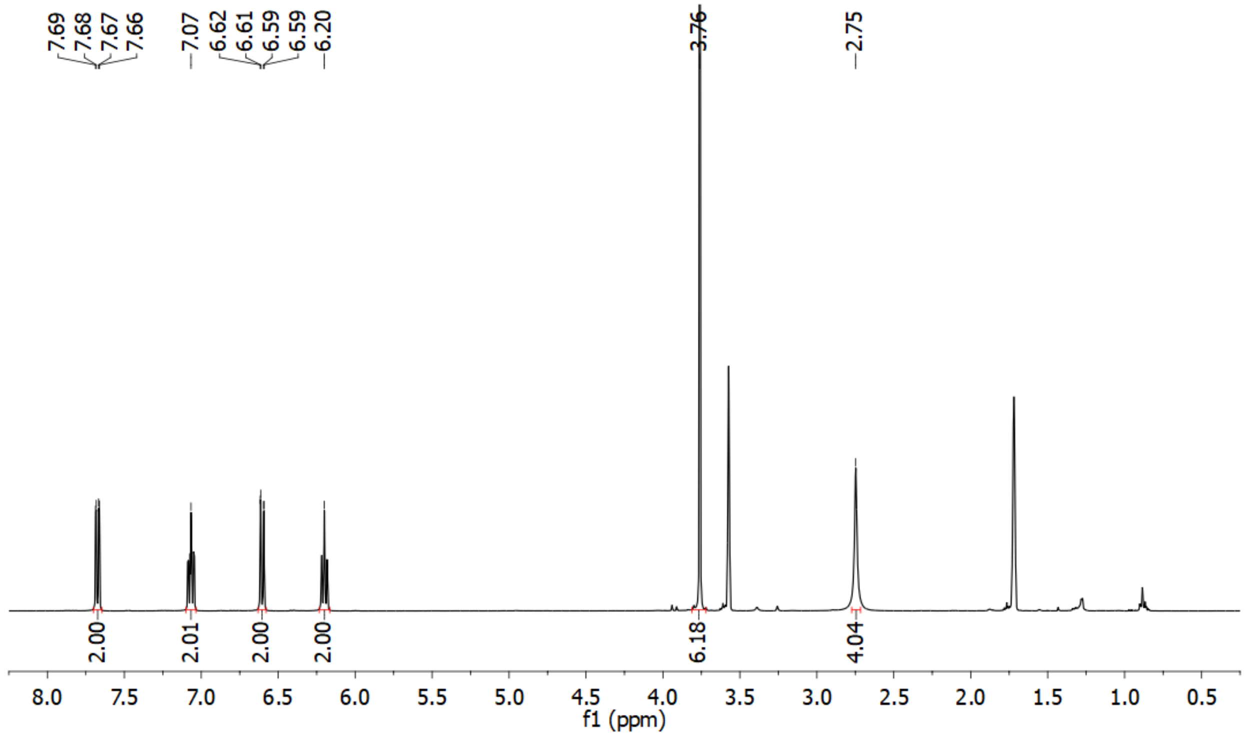

Figure S7. ^{1}H NMR spectrum of **4**.

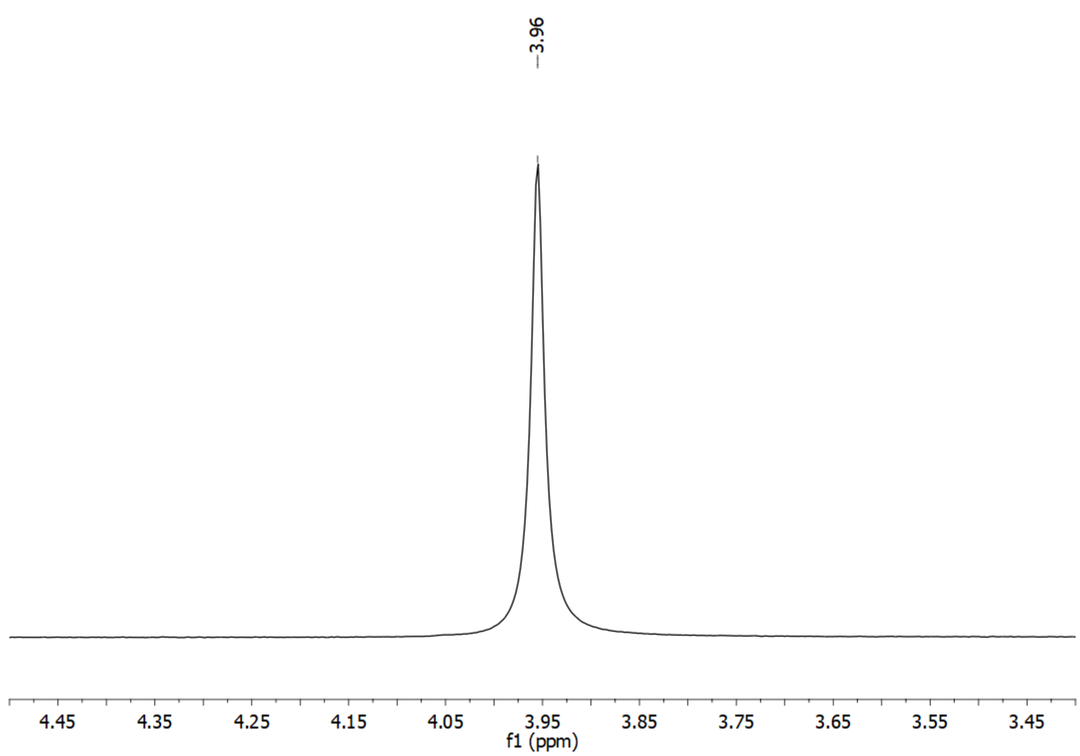

Figure S8. ^{7}Li NMR spectrum of **4**.

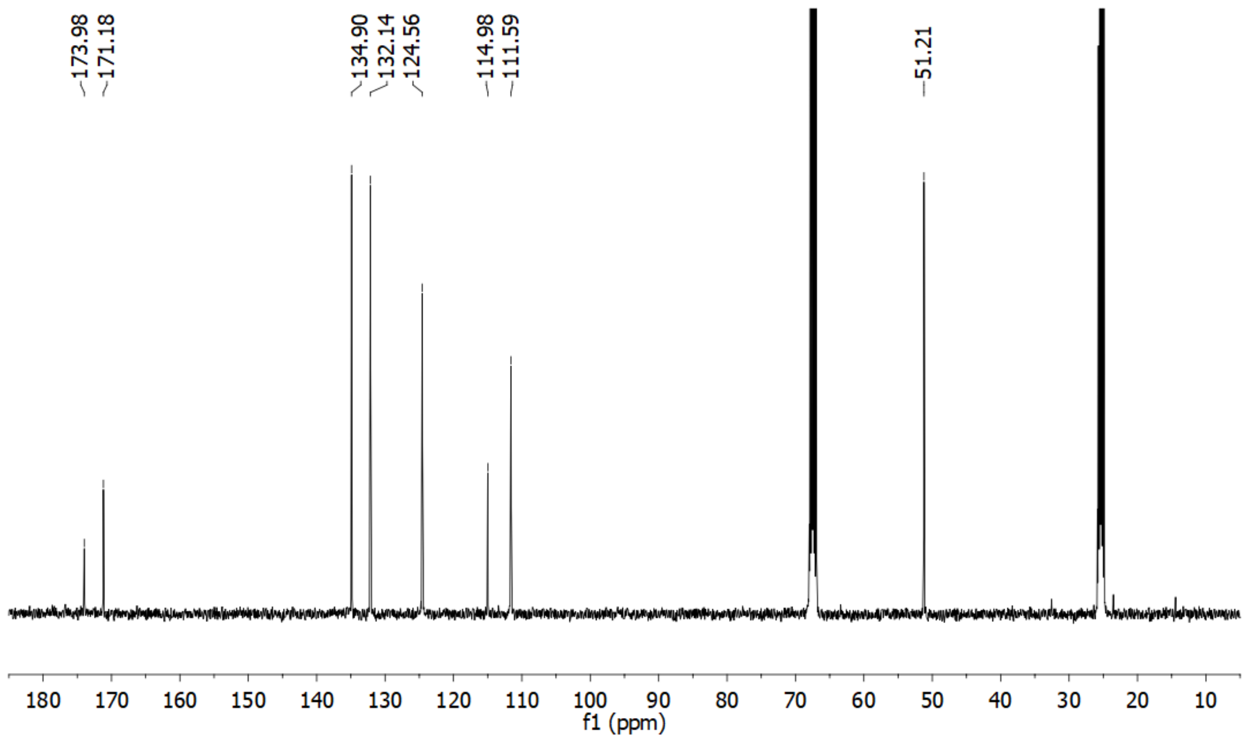

Figure S9. ^{13}C NMR spectrum of **4**.

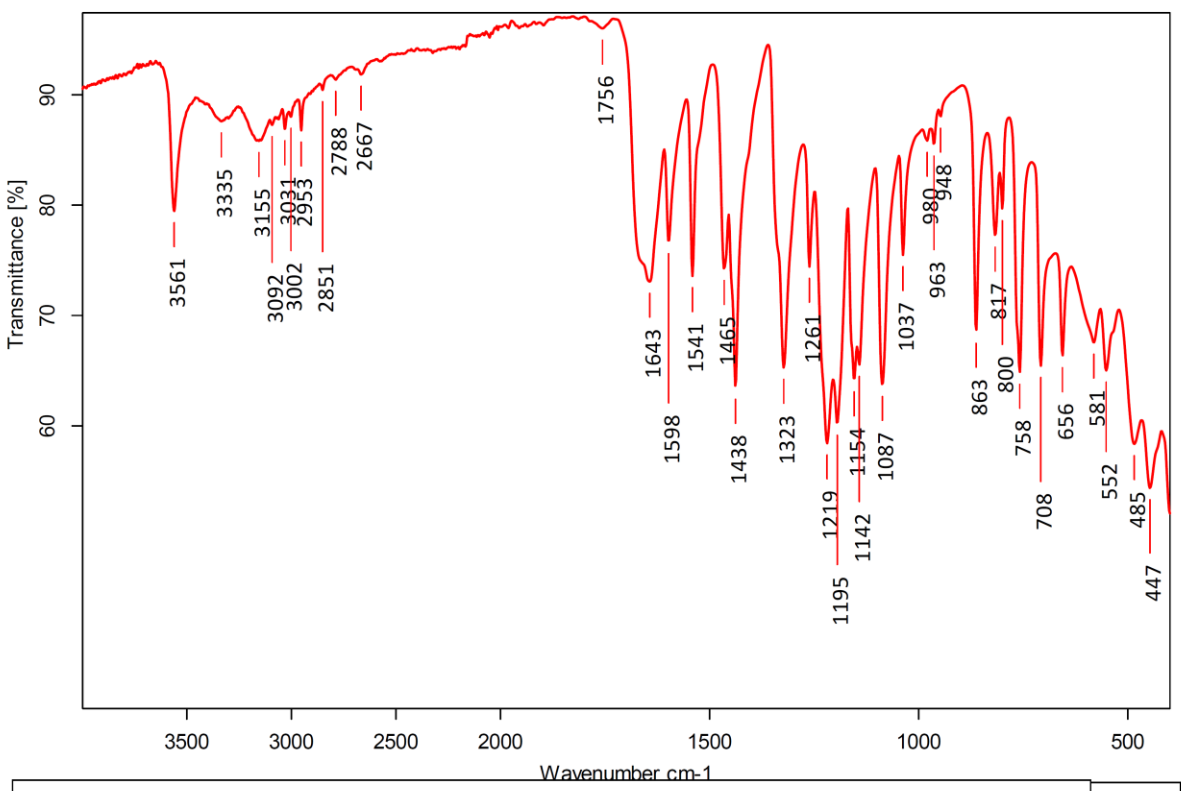

Figure S10. FTIR-ATR spectrum of **4**.

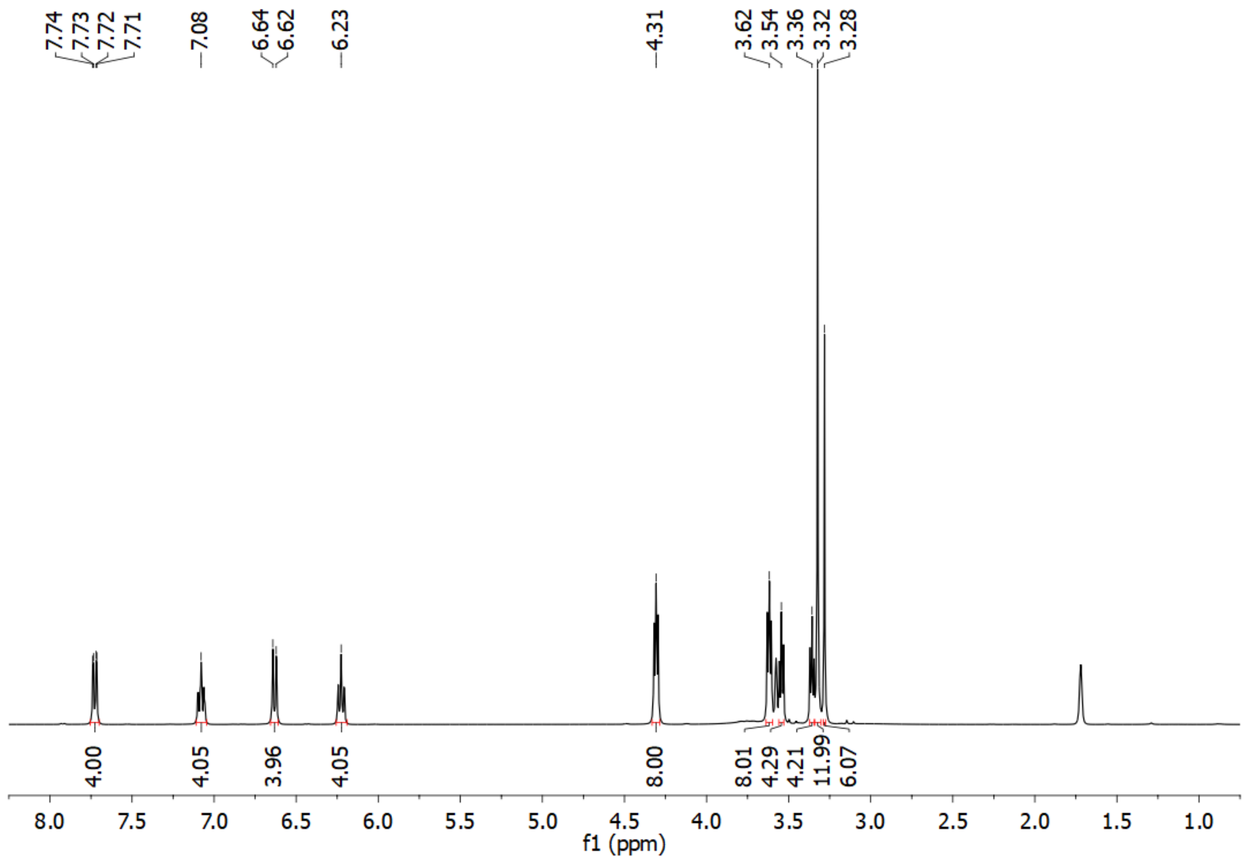

Figure S11. ^{1}H NMR spectrum of **5**.

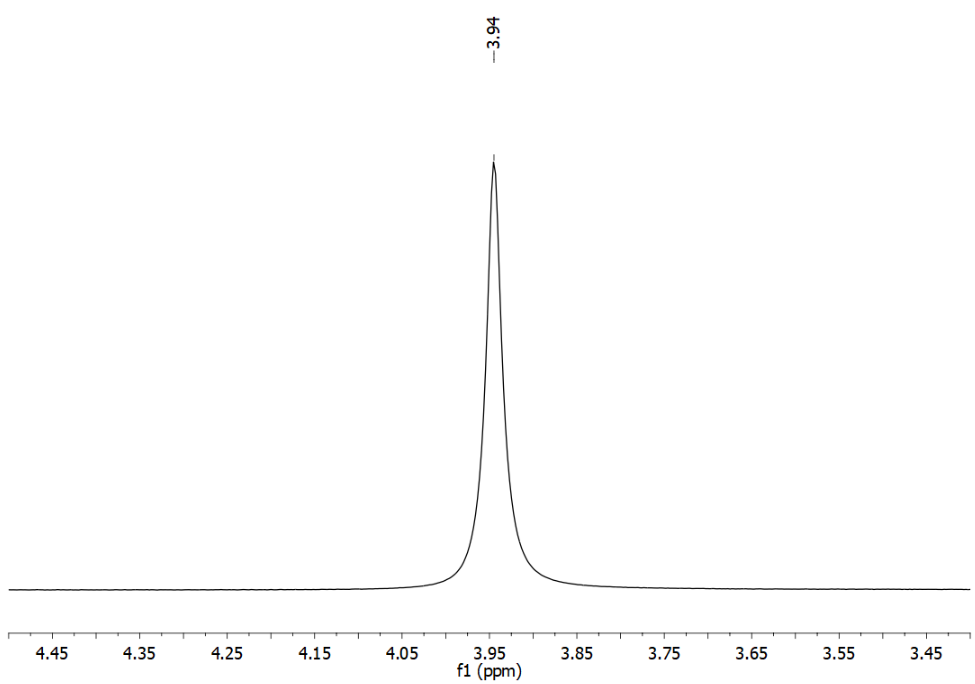

Figure S12. ^{7}Li NMR spectrum of **5**.

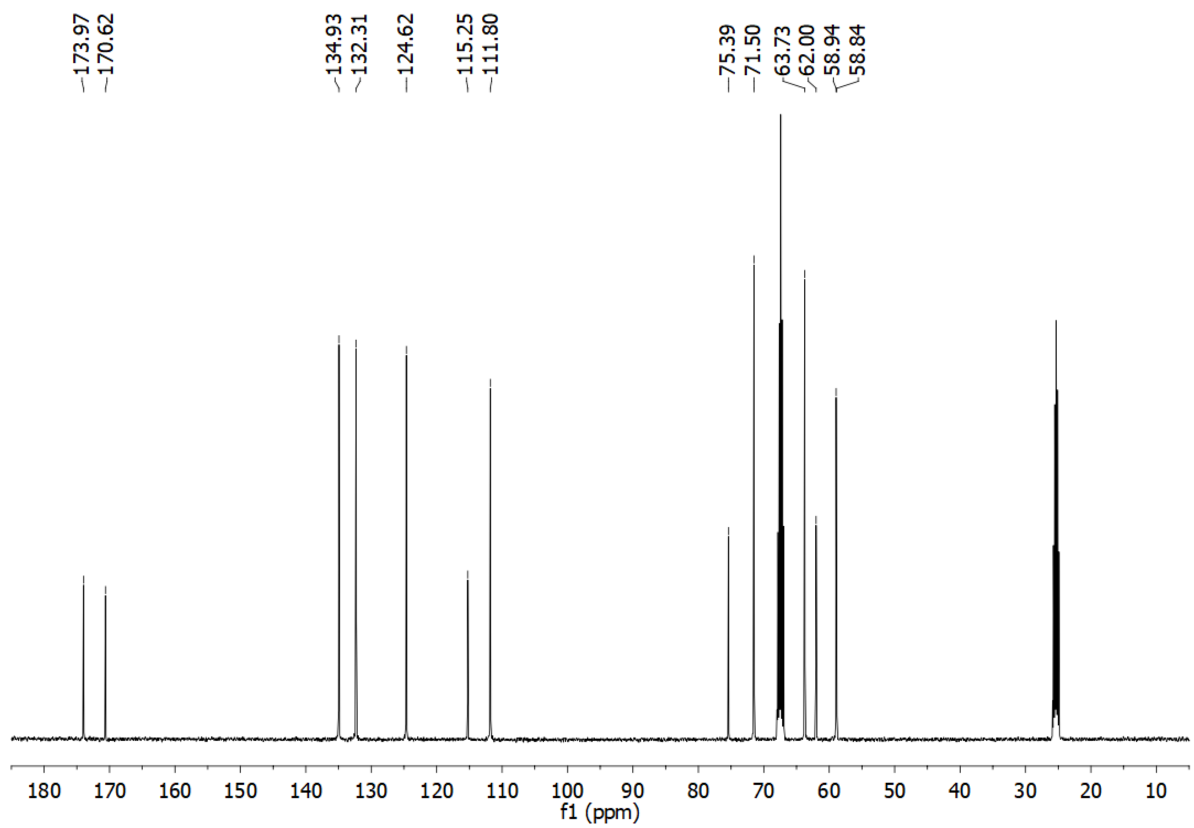

Figure S13. ^{13}C NMR spectrum of **5**.

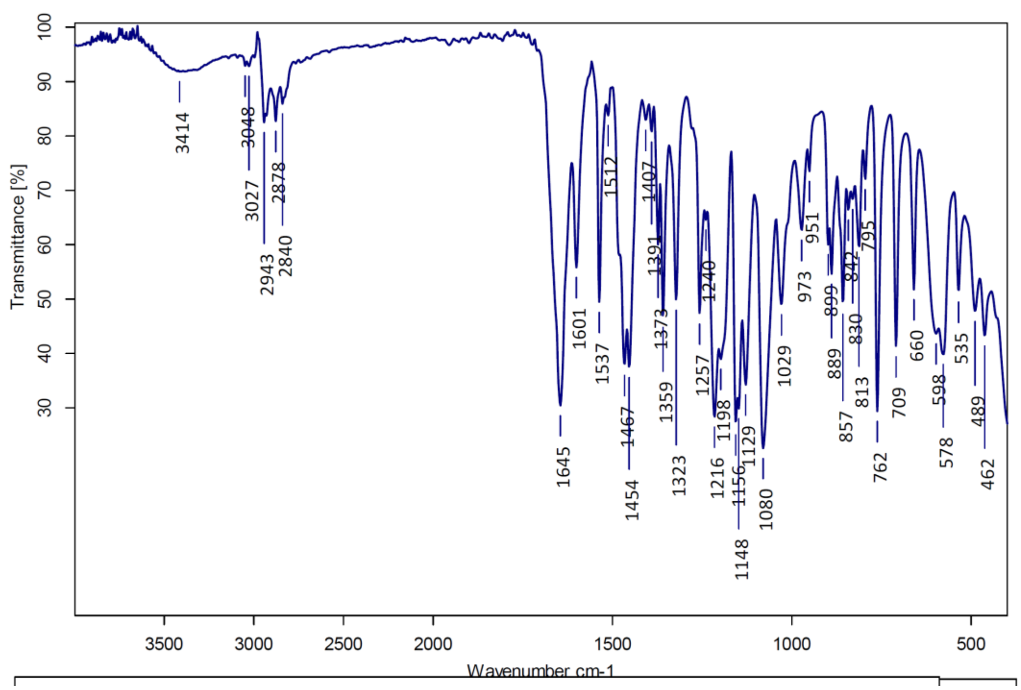

Figure S14. FTIR-ATR spectrum of **5**.

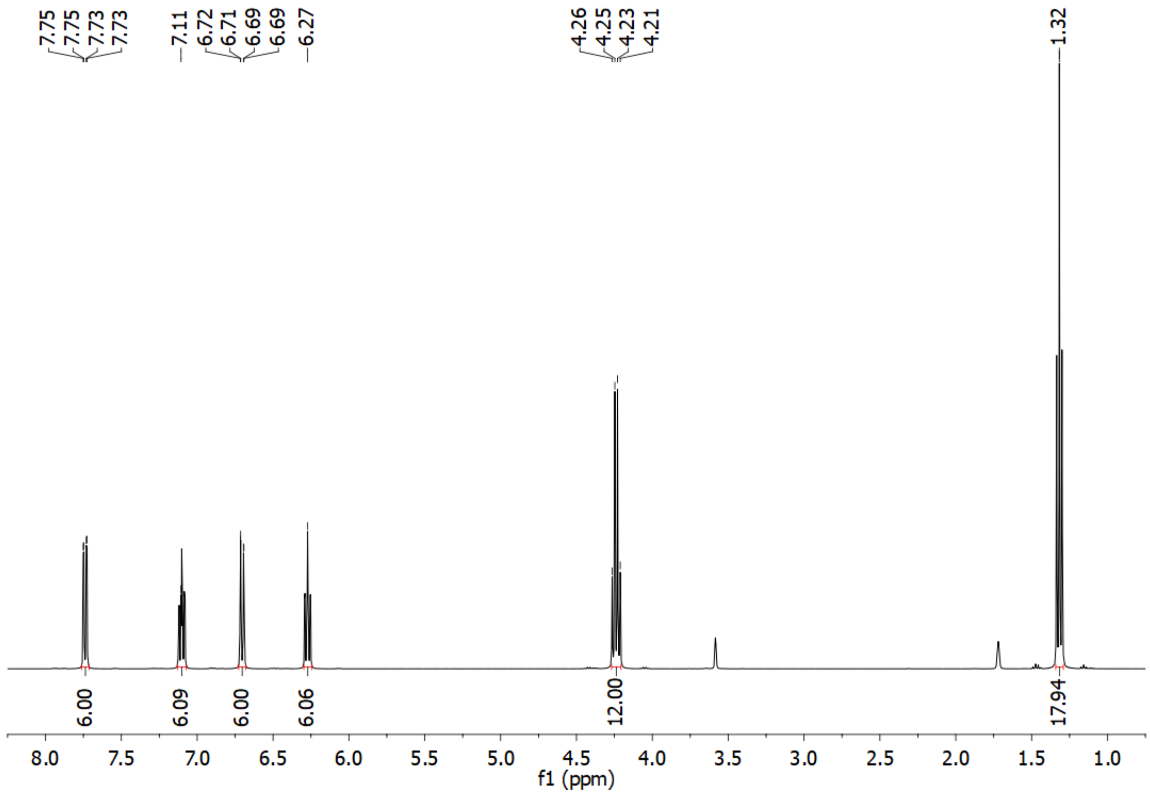

Figure S15. ^{1}H NMR spectrum of **7**.

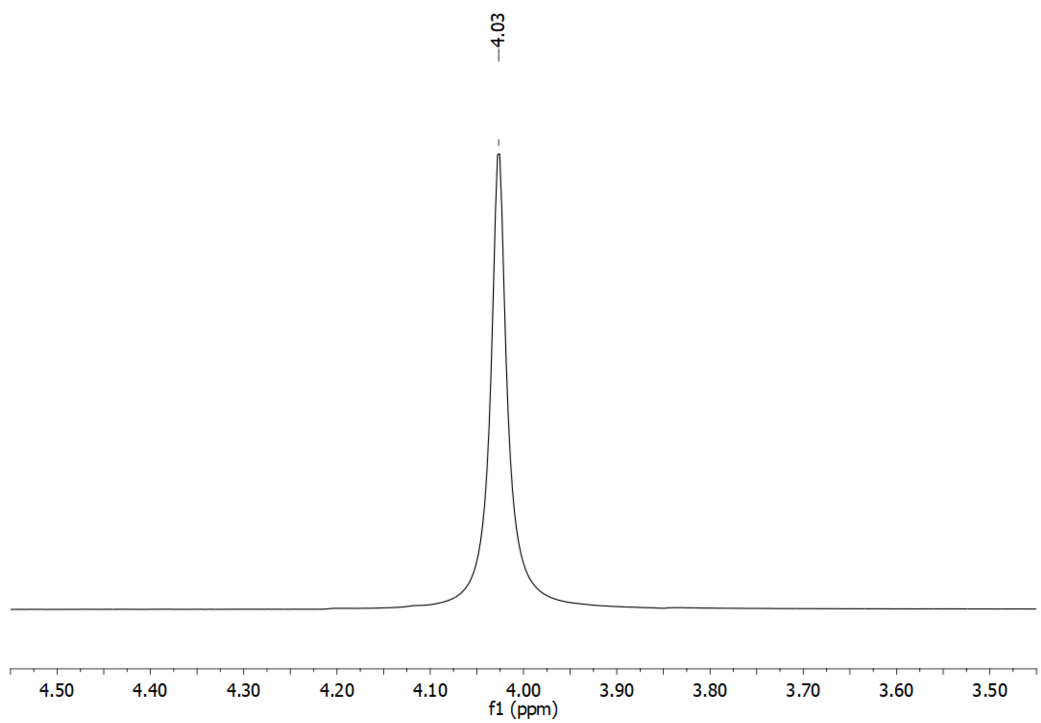

Figure S16. ^{7}Li NMR spectrum of **7**.

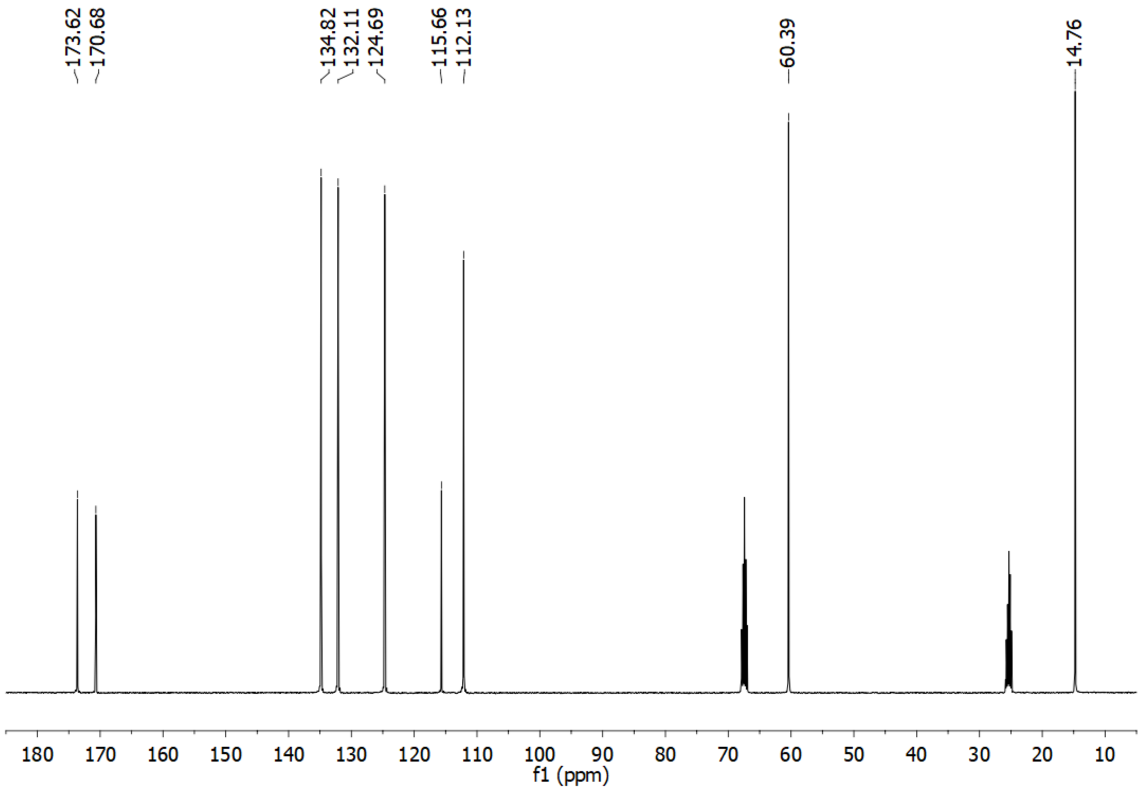

Figure S17. ^{13}C NMR spectrum of **7**.

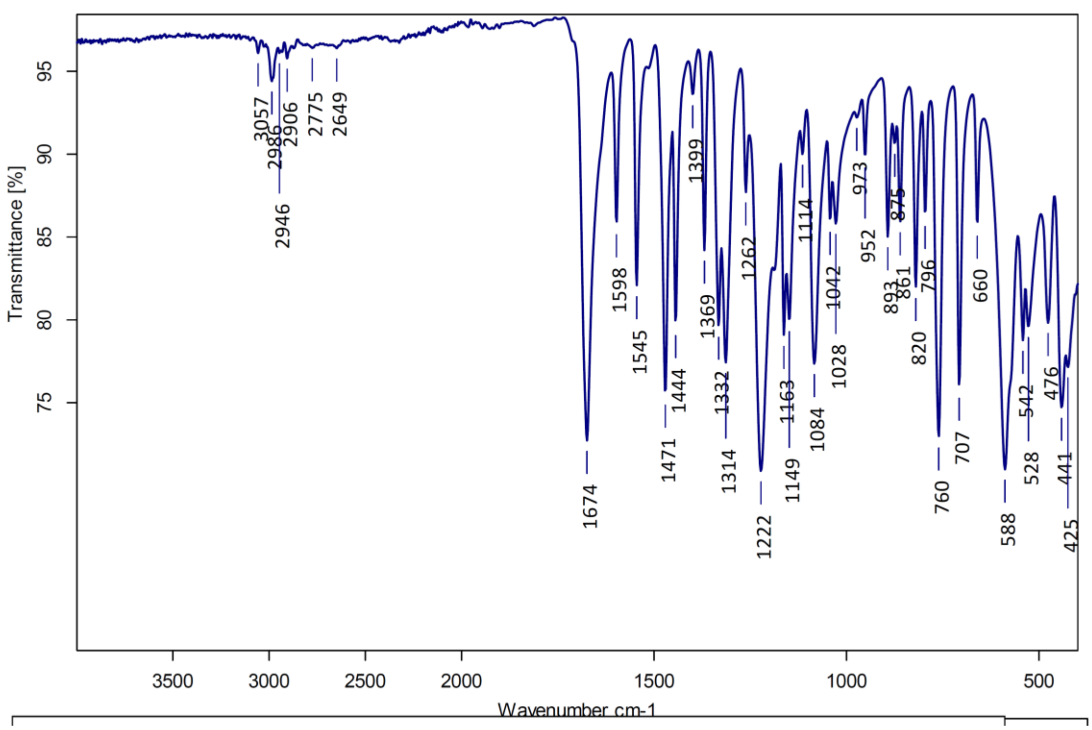

Figure S18. FTIR-ATR spectrum of **7**.

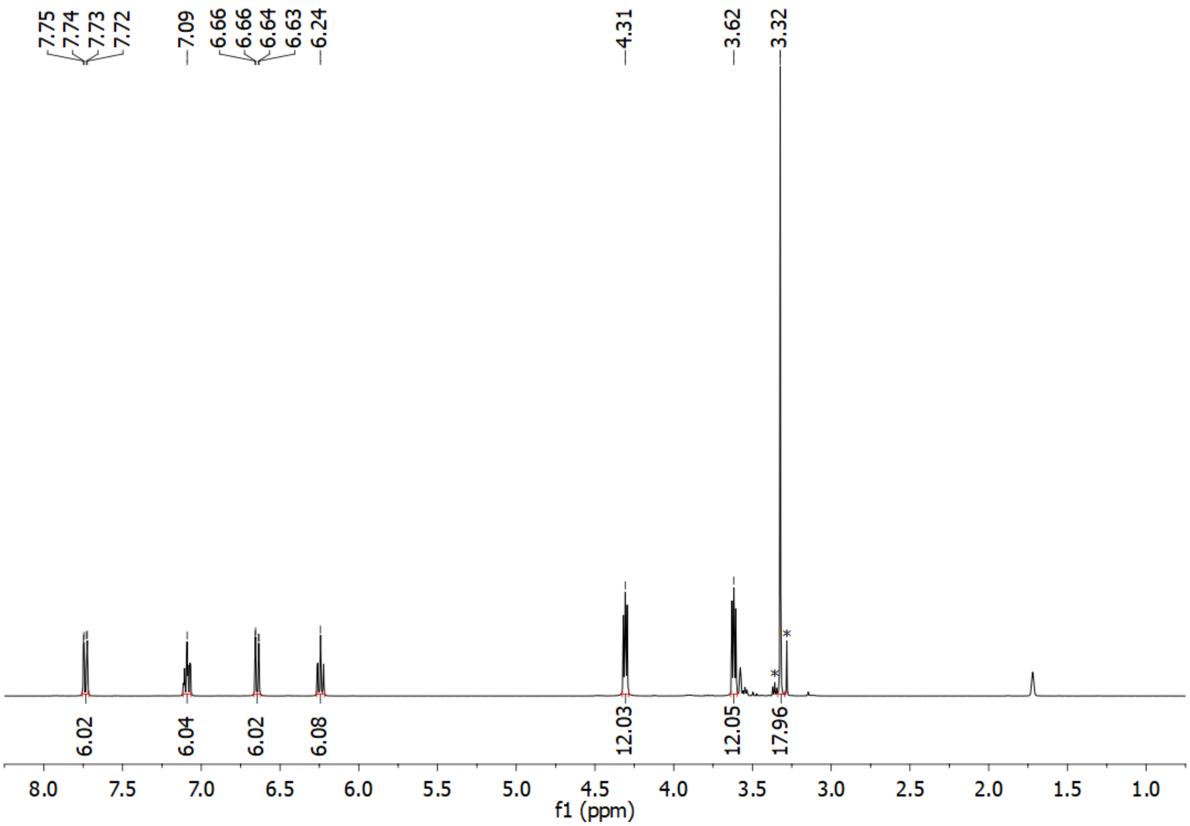

Figure S19. ^{1}H NMR spectrum of **8**. * - assigned EGME residues.

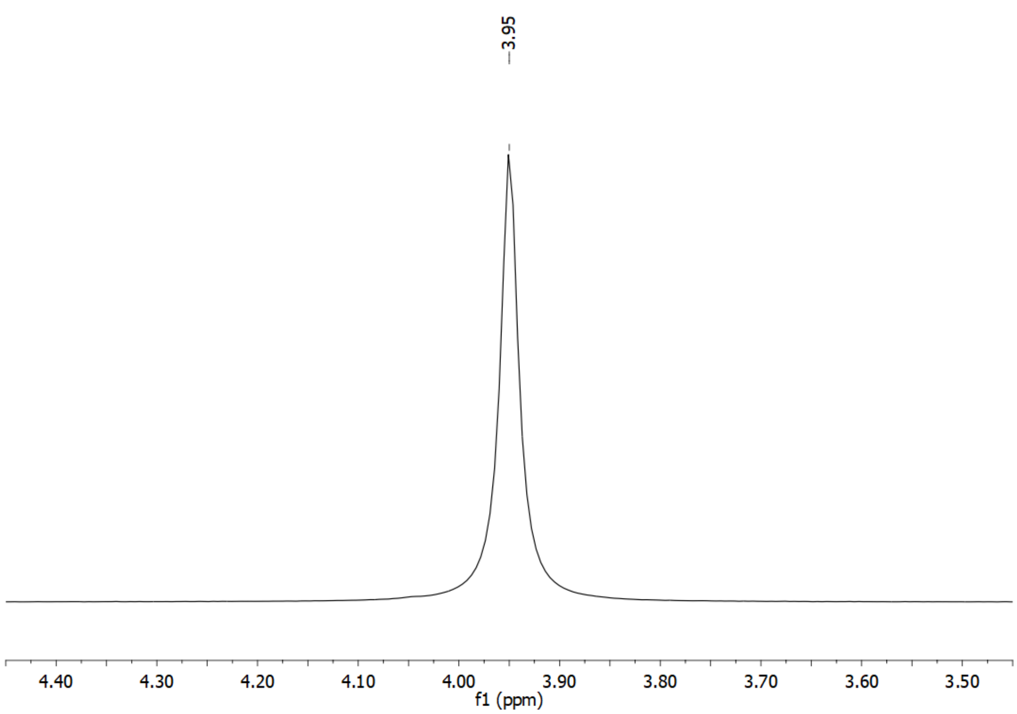

Figure S20. ^{7}Li NMR spectrum of **8**.

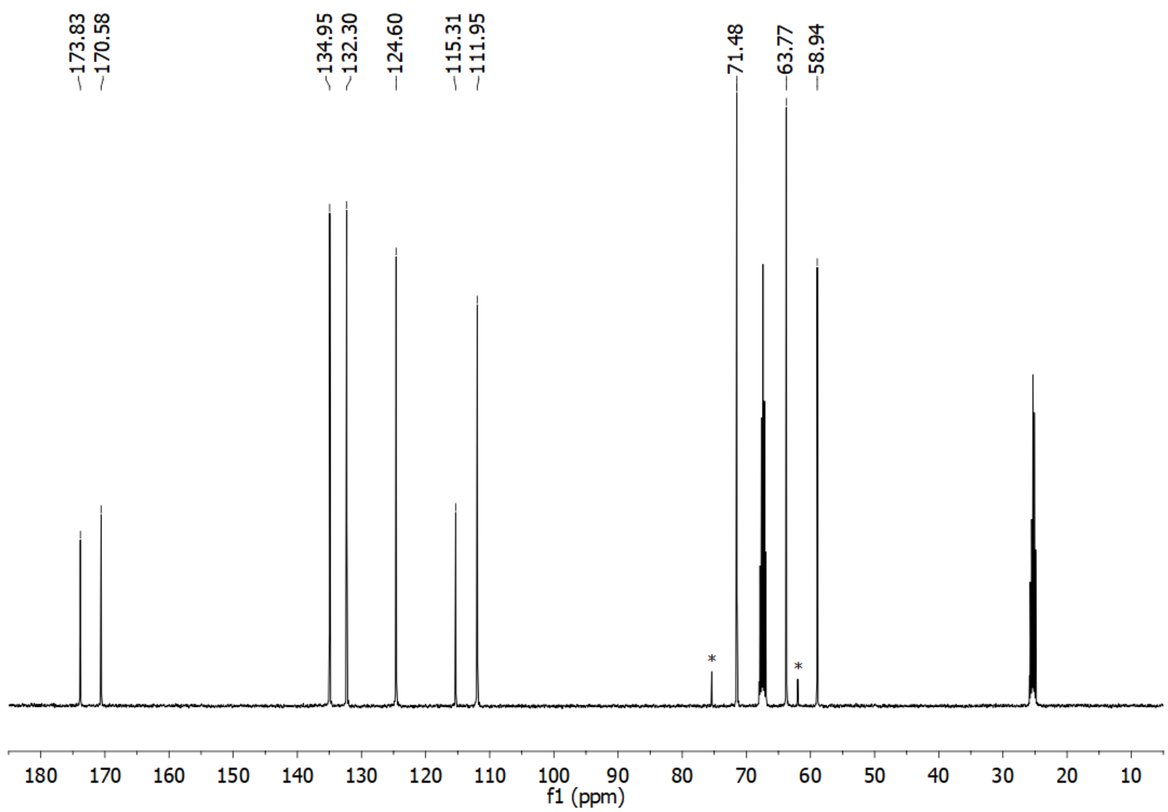

Figure S21. ^{13}C NMR spectrum of **8**. * - assigned EGME residues.

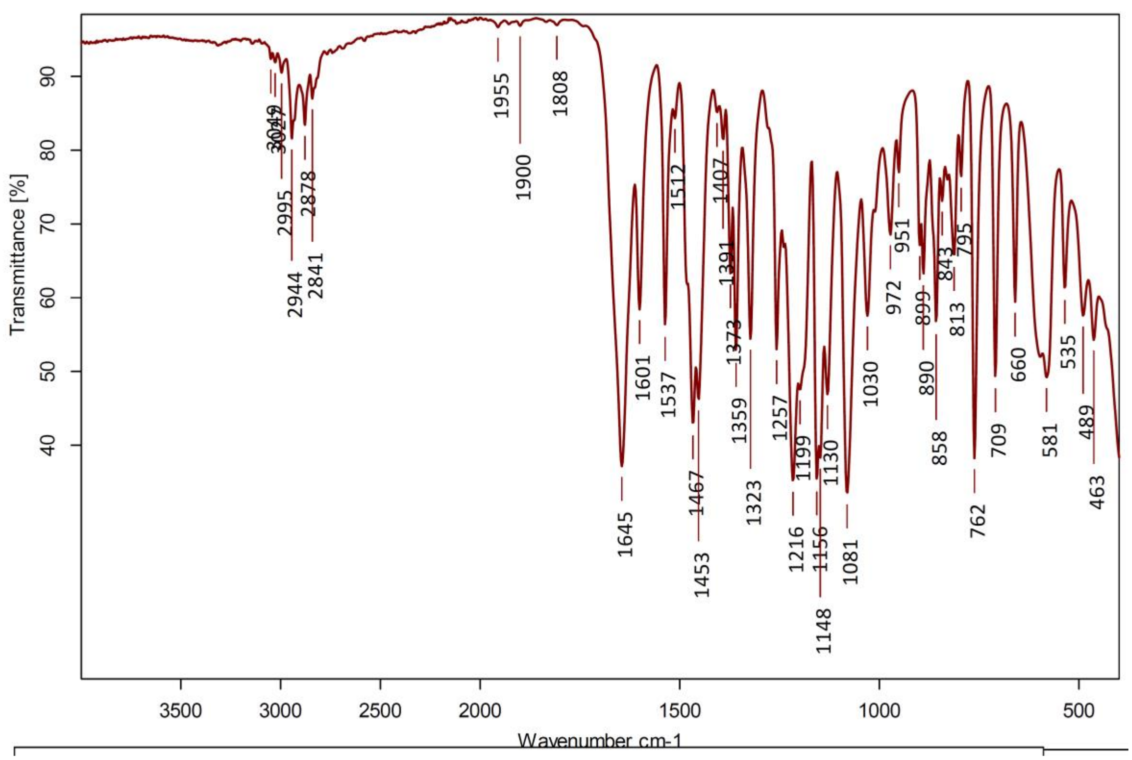

Figure S22. FTIR-ATR spectrum of **8**.

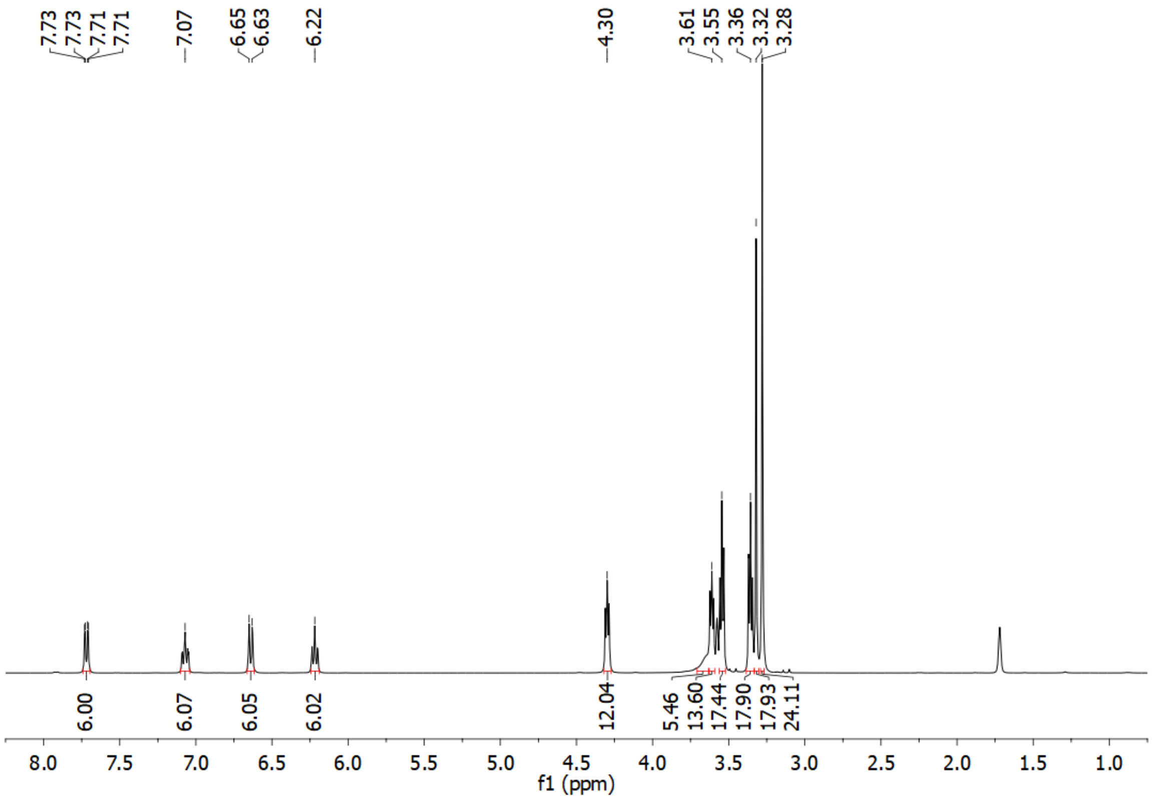

Figure S23. ^{1}H NMR spectrum of **8**·2EGME. After the dissolution of **8**·2EGME the precipitation of **8** upon the excess of alcohol was observed.

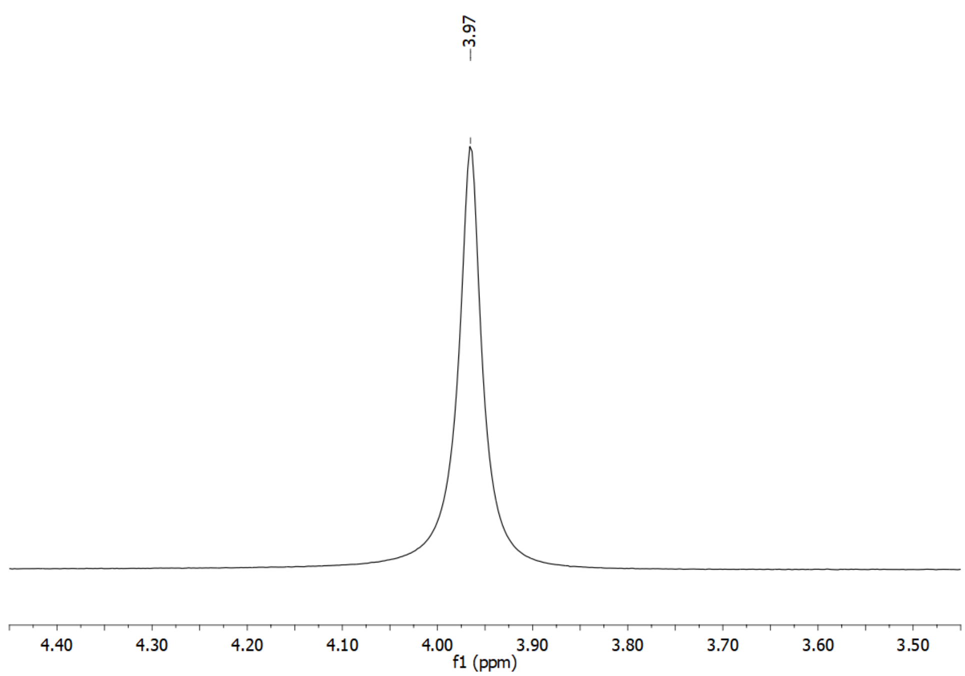

Figure S24. ^{7}Li NMR spectrum of **8**·2EGME.

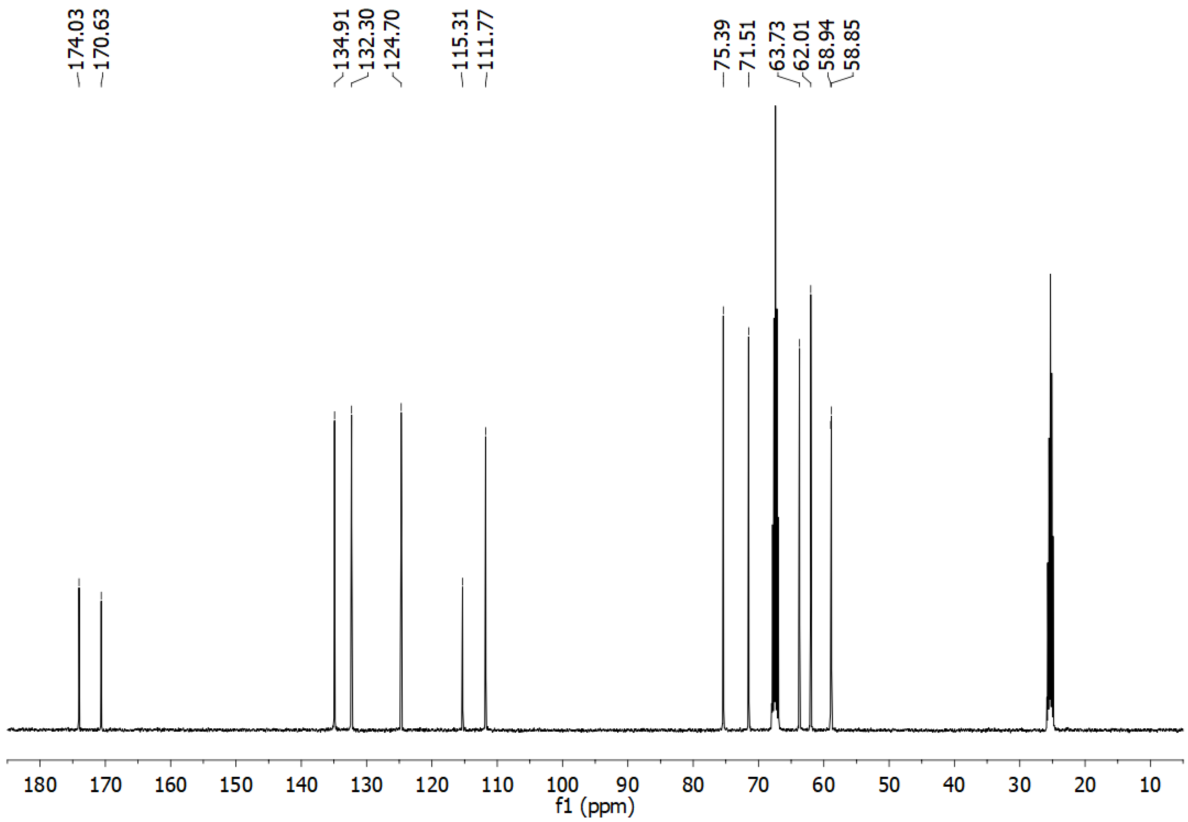

Figure S25. ^{13}C NMR spectrum of **8**·2EGME. After the dissolution of **8**·2EGME the precipitation of **8** upon the excess of alcohol was observed.

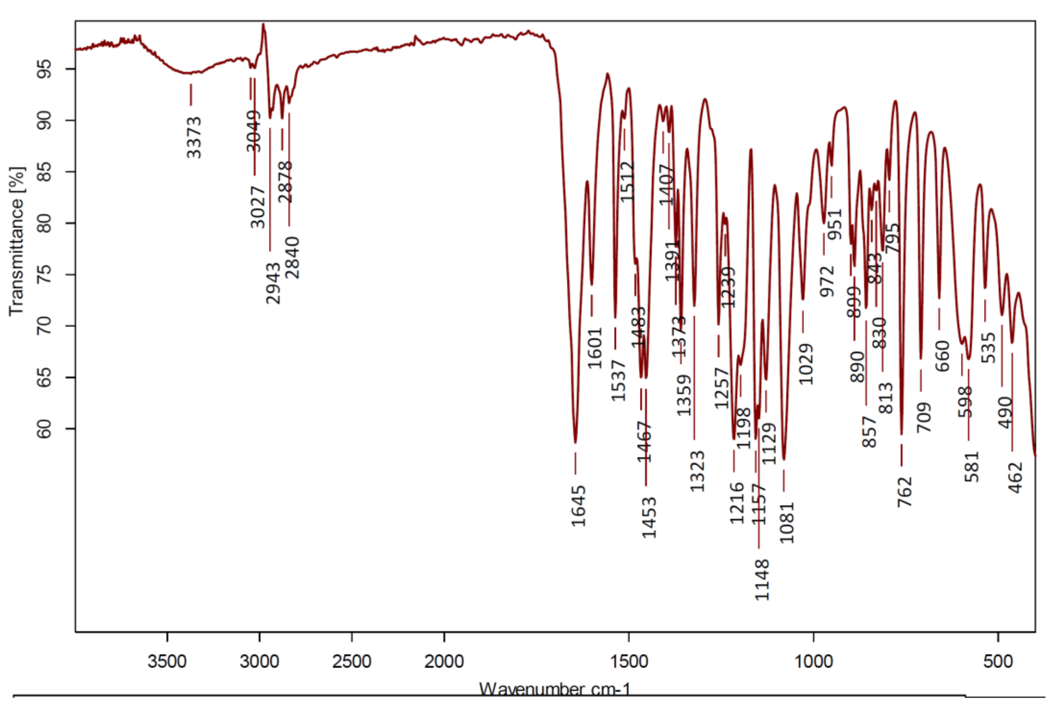

Figure S26. FTIR-ATR spectrum of **8**·2EGME.

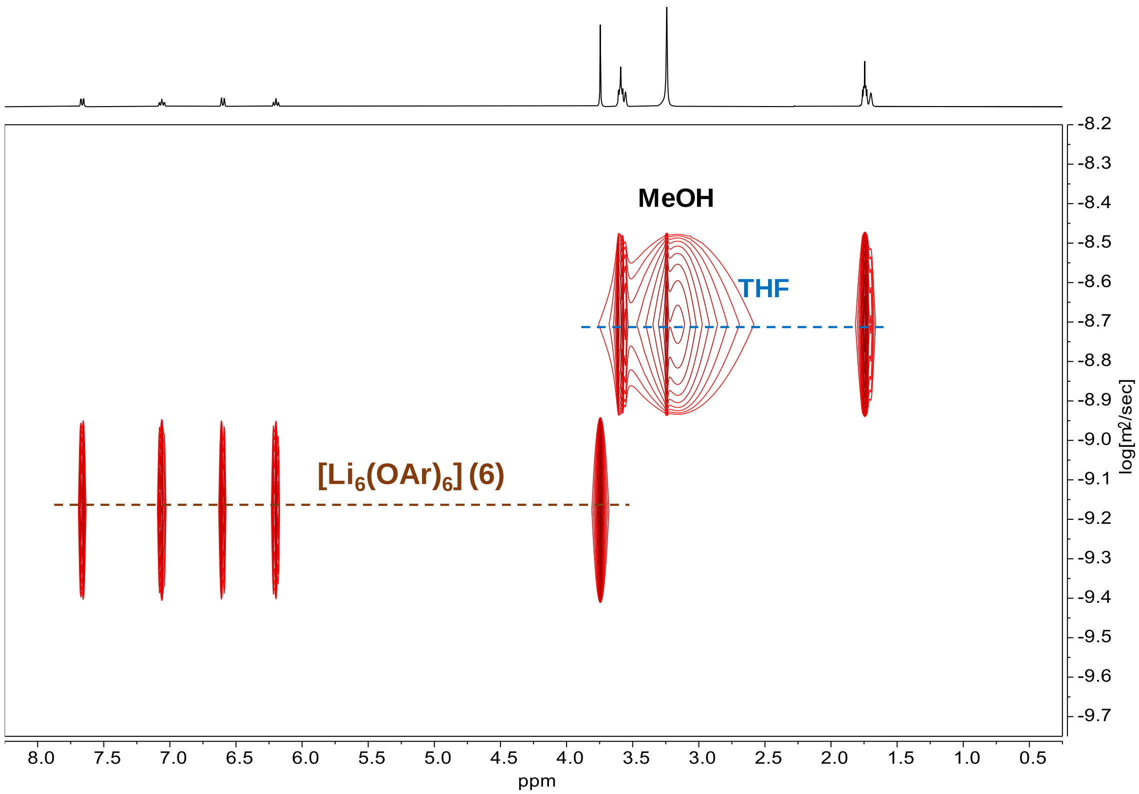

Figure S27. [1]H-DOSY NMR spectrum of **1** in THF-d8.

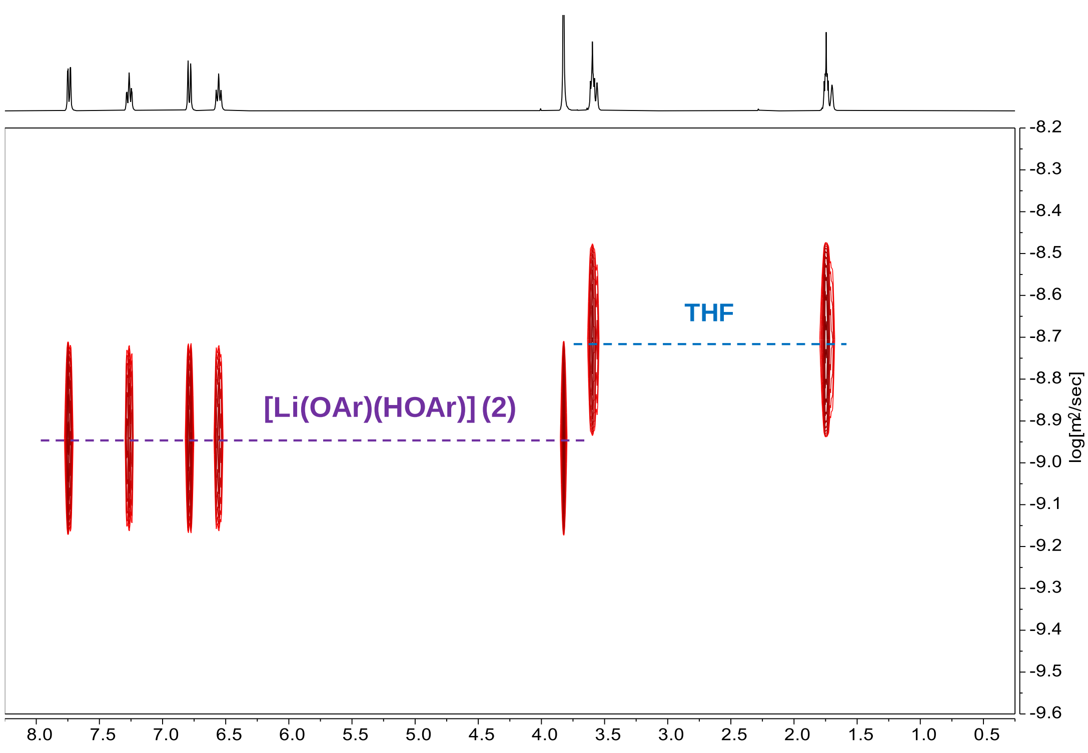

Figure S28. [1]H-DOSY NMR spectrum of **2** in THF-d8.

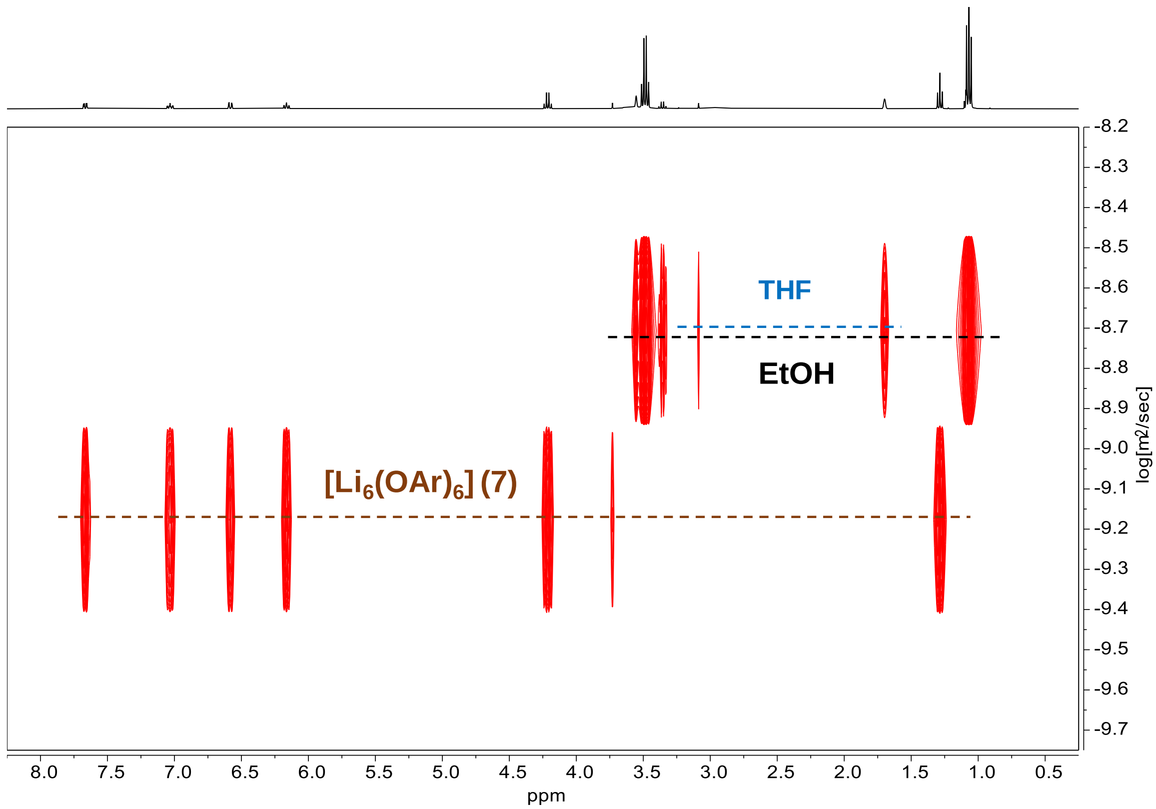

Figure S29. [1]H-DOSY NMR spectrum of **3** in THF-d8.

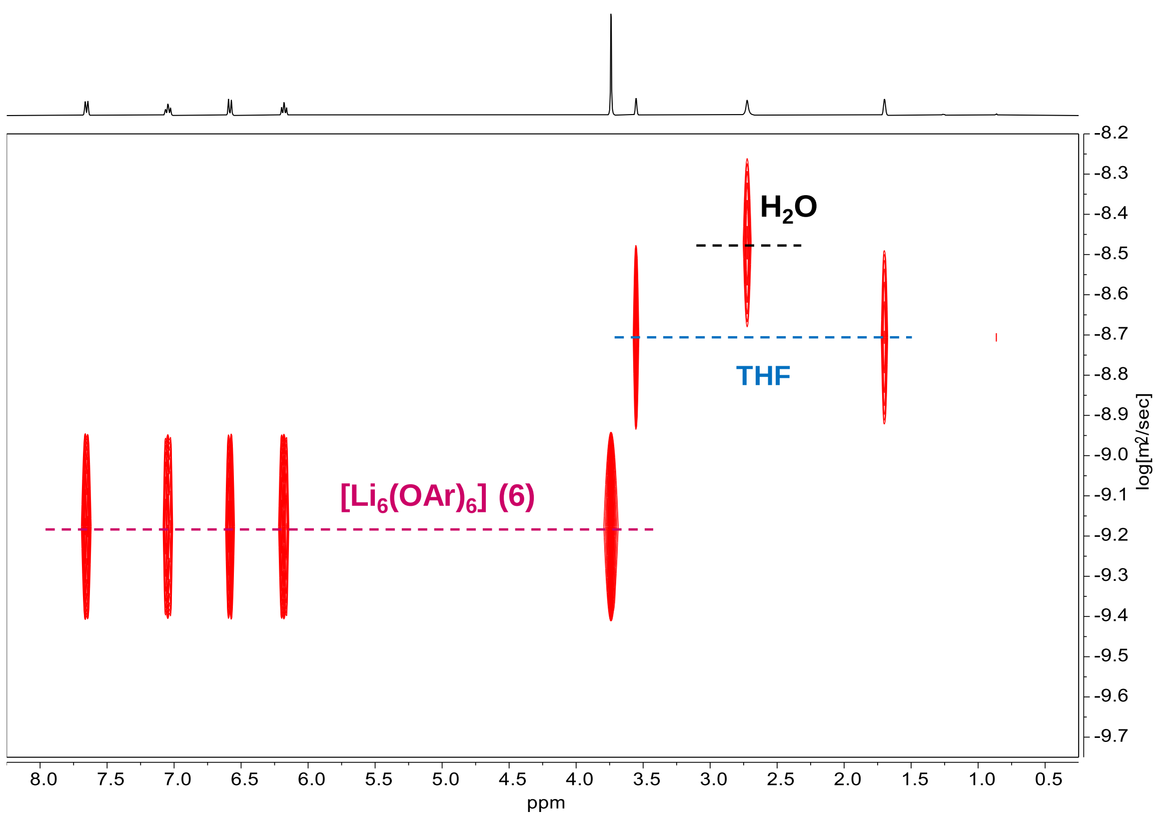

Figure S30. [1]H-DOSY NMR spectrum of **4** in THF-d8.

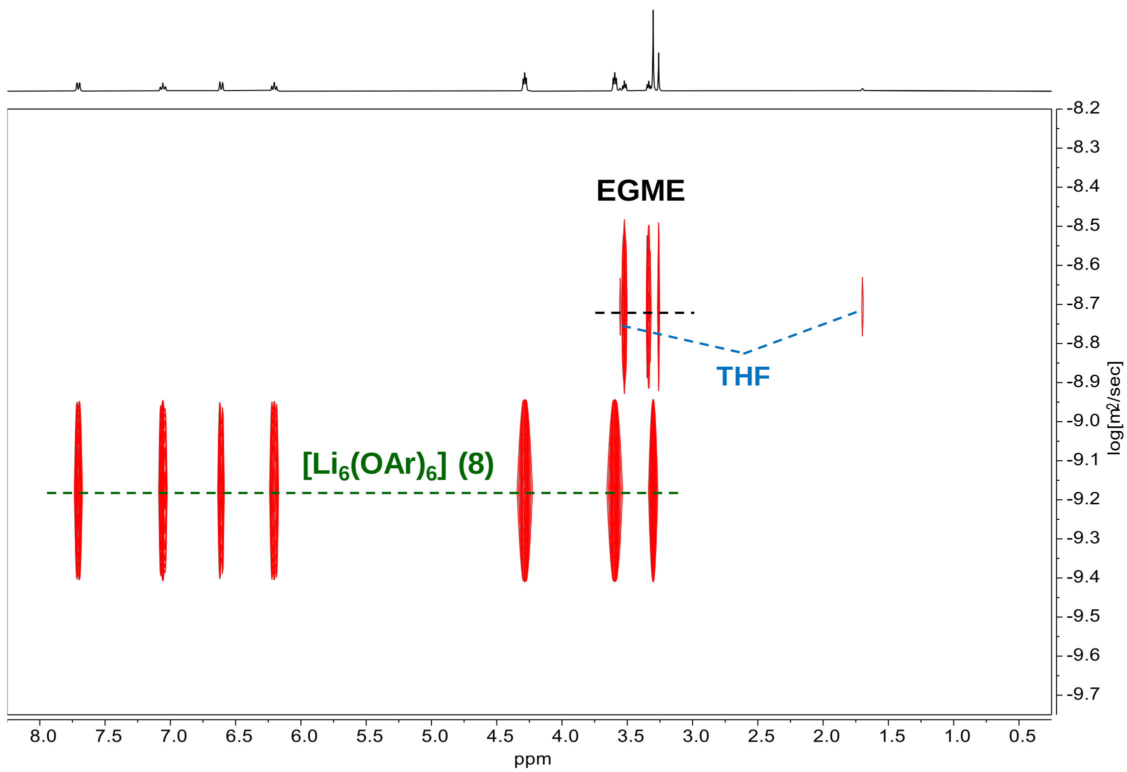

Figure S31. [1]H-DOSY NMR spectrum of **5** in THF-d8.

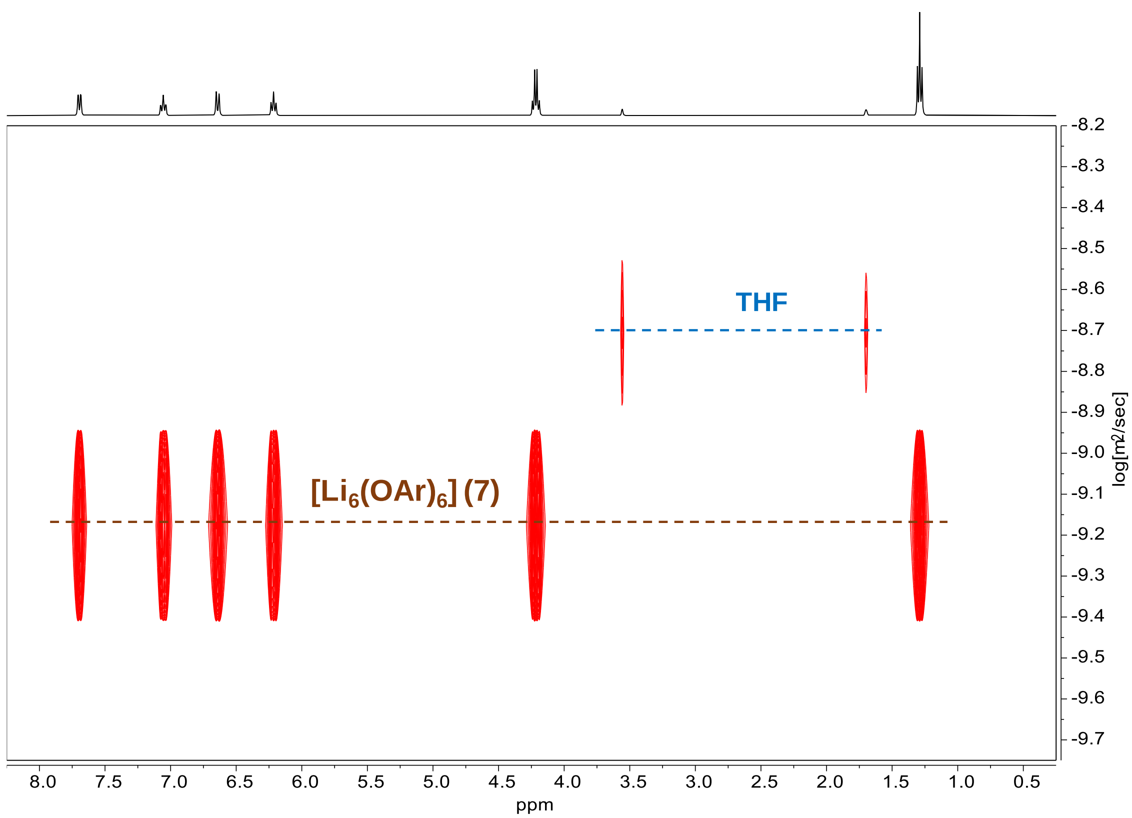

Figure S32. [1]H-DOSY NMR spectrum of **7** in THF-d8.

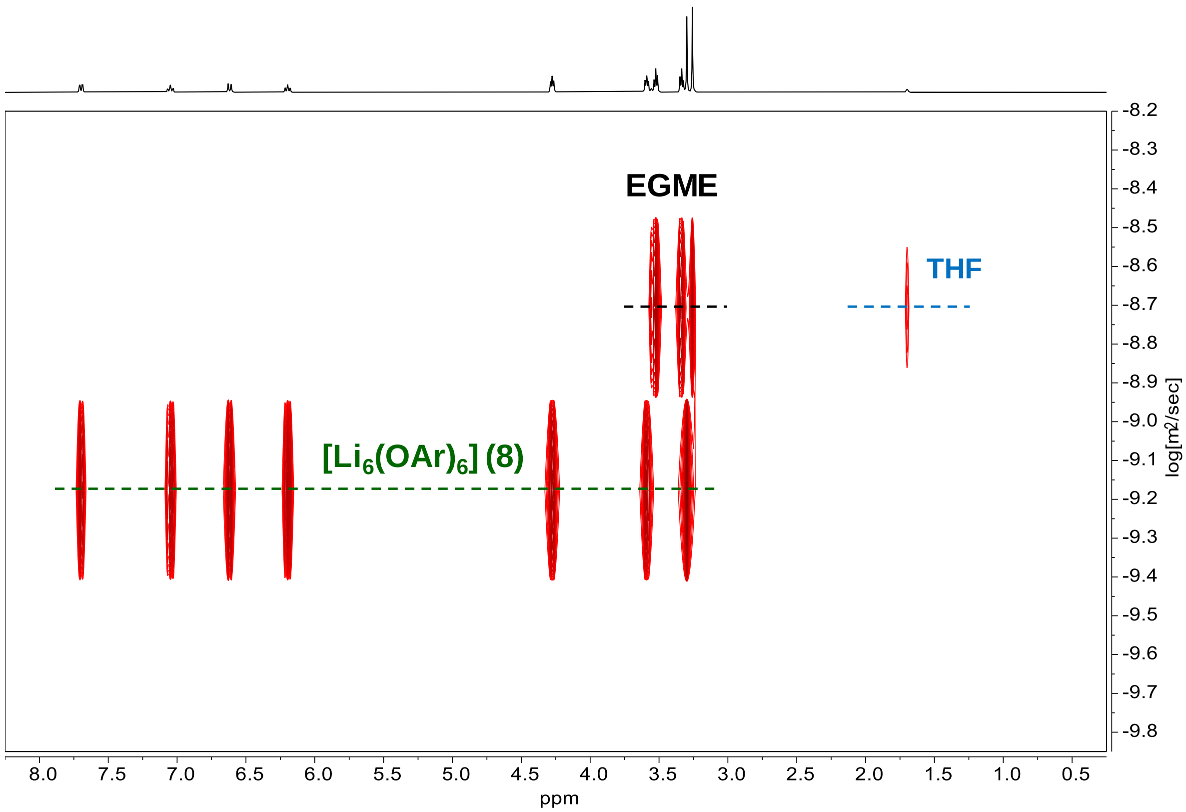

Figure S33. [1]H-DOSY NMR spectrum of **8**·2 EGME in THF-d_8.

Table S3. Formula weights (Fws) and hydrodynamic radii (r_H) of **1** – **8** estimated from the Stokes-Einstein Gierer-Wirtz method.

compound	log(*D*)	T (K)	Fw (g/mol)	Fw_{calc} (g/mol)	$r_{x\text{-}ray}$ (Å)	r_H (Å)
1	-9.172	297.15	222.16 (**1**) 948.48 (**6**)	1006	4.90 (**1**) 7.39 (**6**)	8.60
2	-8.942	297.15	310.23	320	6.24	5.87
3	-9.182	294.95	436.35 (**3**) 1032.64 (**7**)	989	5.62 (**3**) 8.81 (**7**)	8.55
4	-9.175	296.25	352.19 (**4**) 948.48 (**6**)	993	6.26	8.56
5	-9.180	300.45	960.72 (**5**) 1212.80 (**8**)	1164	10.28	9.03
6	-9.160	293.15	948.48	924	7.39	8.36
7	-9.165	300.55	1032.64	1082	8.81	8.89
8·2EGME	-9.181	299.35	1212.80 (**8**) 1364.99 (**8**·2EGME)	1130	9.95	8.94

Table S4. Recovery of lithium from lithium batteries by reaction with methyl salicylate/MeOH.

Battery type	Battery quantity	Li content (g)
PANASONIC CR2430	2	0.09
PANASONIC CR2032	3	0.07
PANASONIC CR2016	1	0.03
GP CR2430	2	0.09
IKEA CR2032	2	0.07
DURACELL CR2032	2	0.07
VARTA CR2032	2	0.07
MAXELL CR2032	1	0.07
TOSHIBA CR2430	1	0.075
TianQiu CR 2032	3	0.057
MULTICOMP CR2032	5	0.07
∑ weight of battery: 78.46 g	∑ 24	∑ 1.686
Recovery compound: **6** - 5.73 g		
Separated cathode material: 29.49 g		
Content of metals in 1g of cathode material: Li - 0.02192g, Mn - 0.4266g		

Table S5. Recovery of lithium from lithium batteries by reaction with methyl salicylate/MeOH.

Battery type	Battery quantity	Li content (g)
CR2430	1	0.09
CR2032	14	0.07
CR2016	1	0.03
∑ weight of battery: 46.21 g	∑ 16	∑ 1.100
Recovery compound: **6** - 10.36 g		
Separated cathode material: n.d. g		
Content of metals in 1g of cathode material: Li - 0.02418 g, Mn - 0.41389 g		

Table S6. Recovery of lithium from lithium batteries by reaction with methyl salicylate/MeOH.

Battery type	Battery quantity	Li content (g)
PANASONIC CR2430	11	0.09
ROHSCELL 2430	1	0.09
GP CR2430	2	0.09
TOSHIBA CR2430	11	0.075
∑ weight of battery: 108.5 g	∑ 25	∑ 2.085
Recovery compound: **6** - 3.46 g, Li_2CO_3 - 4.46 g		
Separated cathode material: 37.81 g		
Content of metals in 1g of cathode material before Li_2CO_3 and $LiClO_4$ isolation: Li - 0.03128 g, Mn - 0.4554 g.		

Table S7. Recovery of lithium from lithium batteries by reaction with methyl salicylate/^{i}PrOH.

Battery type	Battery quantity	Li content (g)
MITSHUBISI CR2032E	1	0.064
MAXELL CR2032	3	0.07
MULTICOMP CR2032	4	0.07
IKEA CR2032	6	0.07
PANASONIC CR2032	4	0.07
VARTA CR2032	5	0.07
∑ weight of battery: 69.66 g	∑ 23	∑ 1.604
Recovery compound: **2** - 14.64 g		

Table S8. Recovery of lithium from lithium batteries by reaction with methyl salicylate/$EtOH_{(anhydrous)}$.

Battery type	Battery quantity	Li content (g)
IKEA CR2032	4	0.07
MITSHUBISI CR2032E	1	0.064
MAXELL CR2032	6	0.07
MULTICOMP CR2032	1	0.07
ENERGIZER 2032	3	0.109
2032	7	0.07
2025	2	0.048
2016	1	0.023
T&E 2032	1	0.07
∑ weight of battery: 74.22 g	∑ 26	∑ 1.840
Recovery compound: **7** - 12.1 g, Li_2CO_3 - 2.98 g		
Separated cathode material: 24.07 g		
Content of metals in 1g of cathode material before Li_2CO_3 and $LiClO_4$ isolation: Li - 0.01813 g, Mn - 0.41026 g.		

Table S9. Recovery of lithium from lithium batteries by reaction with methyl salicylate/EGME.

Battery type	Battery quantity	Li content (g)
2032	10	0.07
MAXELL CR2032	1	0.07
ENERGIZER 2032	1	0.109
IKEA CR2032	1	0.07
DURACELL 2032	1	0.07
TOSHIBA 2032	1	0.07
FREEGO 2032	2	0.066
VARTA 2032	1	0.07
VINNIC 2032	1	0.07
RUBIN 2032	1	0.07
∑ weight of battery: 58.66 g	∑ 20	∑ 1.431
Recovery compound: **5** - 16.71 g		

Table S10. Recovery of lithium from primary lithium battery anodes by reaction with H_2O.

Battery type	Battery quantity	Li content (g)
PANASONIC CR2032	4	0.07
MITSUBISHI CR2032	1	0.064
MAXELL CR2032	7	0.07
ENERGIZER 2032	7	0.109
SONY 2032	5	0.07
∑ weight of battery: 70.50 g	∑ 24	∑ 1.947
Recovery compound: $LiOH{\cdot}H_2O$ - 2.15 g, Li_2CO_3 - 2.01 g		
Separated cathode material: 27.24 g		
Content of metals in 1g of cathode material before Li_2CO_3 and $LiClO_4$ isolation: Li - 0.02865 g, Mn - 0.4074 g.		
Content of Li in 1g of cathode material after Li_2CO_3 and $LiClO_4$ isolation: Li - 0.00689 g.		

Table S11. Recovery of lithium from primary lithium battery anodes by reaction with methyl salicylate.

Battery type	Battery quantity	Li content (g)
Varta CR123A,	3	0.58
Duracell Ultra CR2	1	0.30
∑ weight of battery: 61.37 g	∑ 4	∑ 2.04
Recovery compound: **2** - 11.20 g		

Table S12. Recovery of lithium from primary lithium battery anodes by reaction with methyl salicylate/EtOH$_{(hydrous)}$.

Battery type	Battery quantity	Li content (g)
AAA$^+$ Energizer lithium	16	0.5
∑ weight of battery: 120.38 g	∑ 16	∑ 8.0
Recovery compound: **4** - 78.60 g or **7** - 64.80 g		

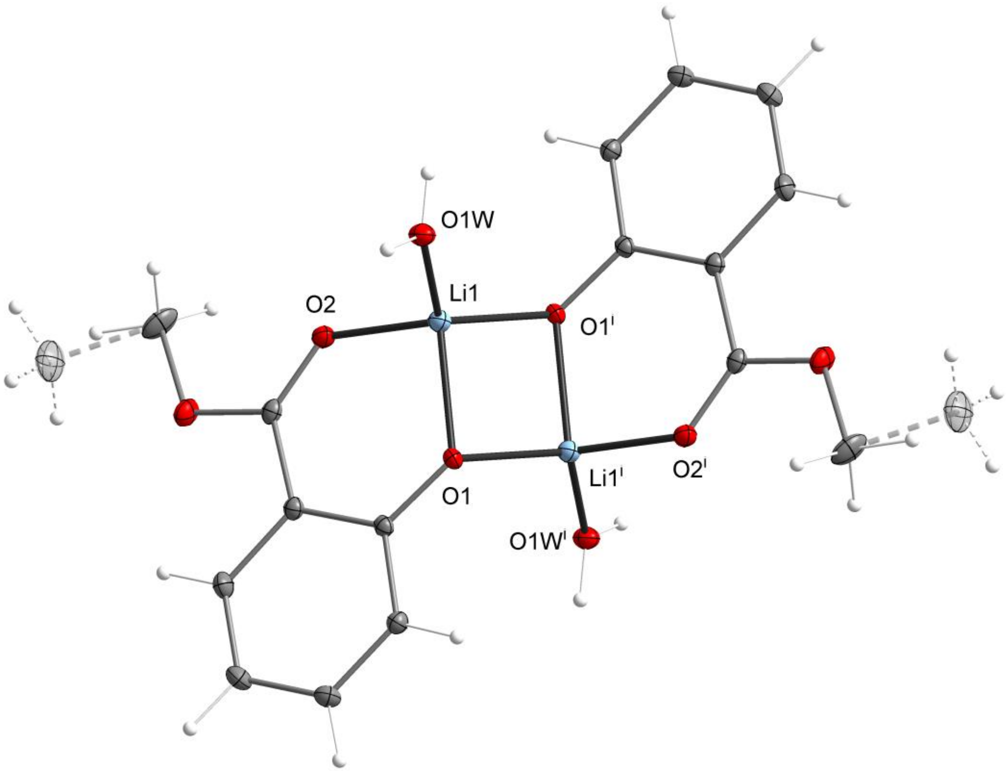

Figure S34. Molecular structure of [Li(OAr)(H_2O)]$_2$ (**4a**) for ArOH = methyl salicylate (0.6), ethyl salicylate (0.4). Displacement ellipsoids are drawn at the 25% probability level. [symmetry code: (i) $-x$+0.5, $-y$+1.5, $-z$]. The structure contains disorder aromatic ligand molecules ArO$^-$ = methyl salicylate (0.6), ethyl salicylate (0.4).

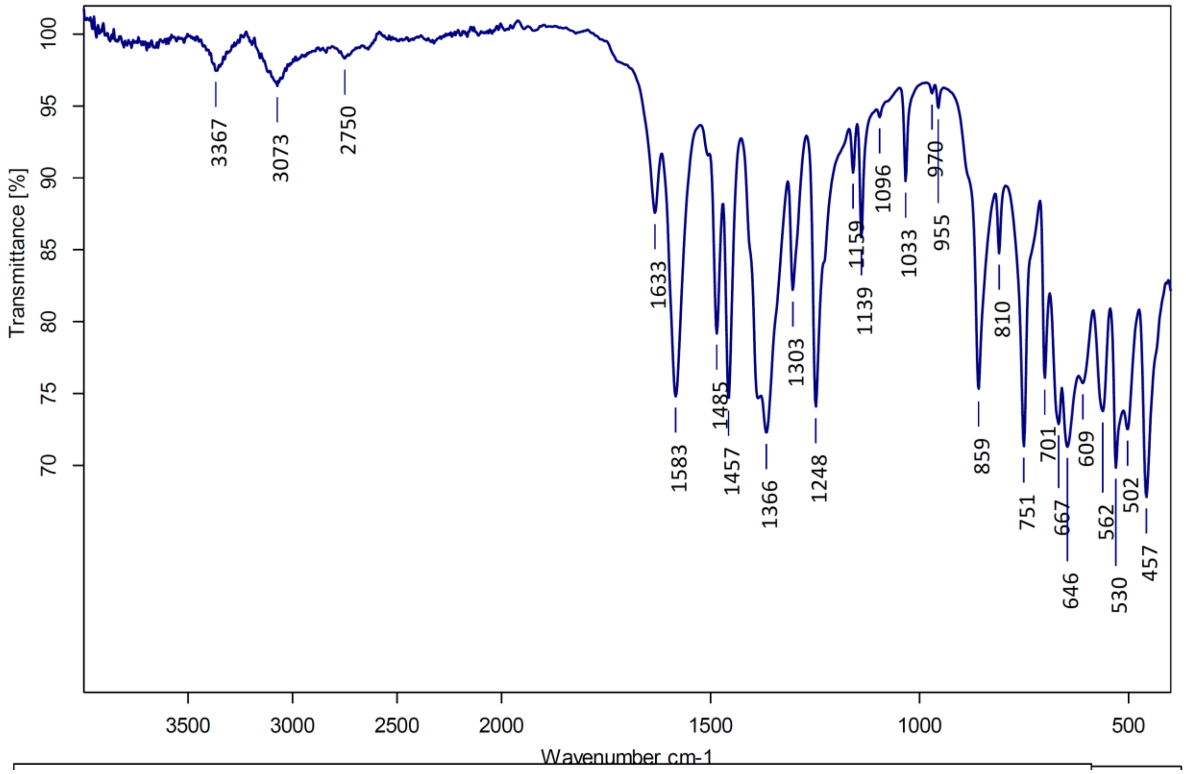

Figure S35. FTIR-ATR spectrum of **10**.

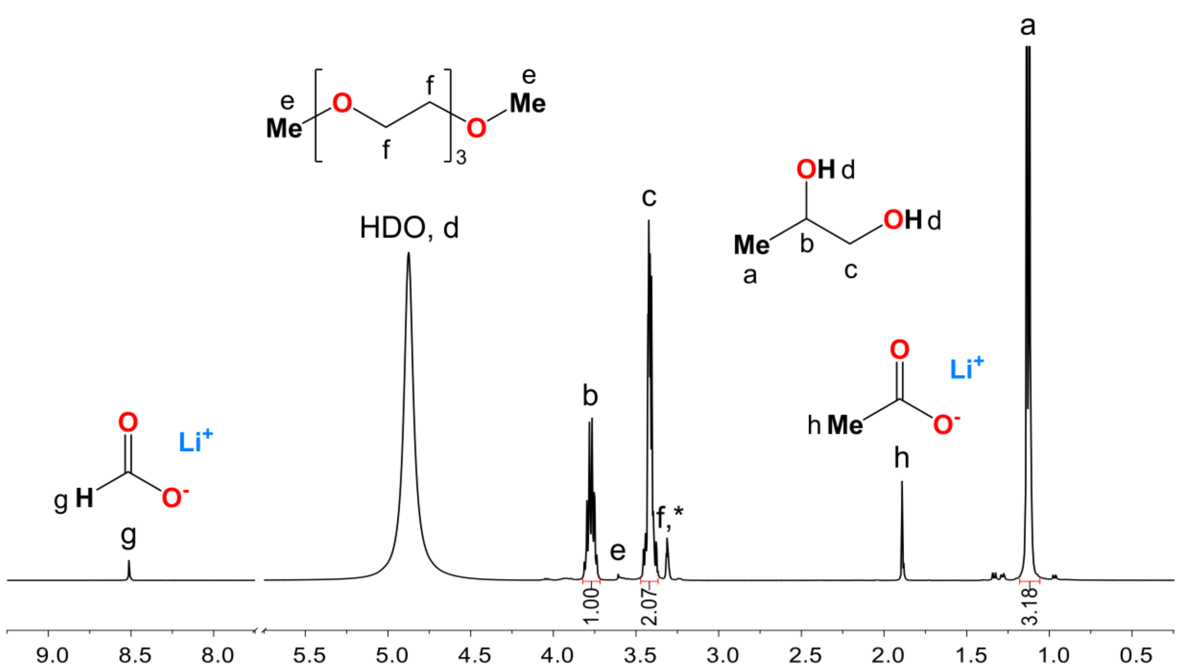

Figure S36. [1]H NMR spectrum in CD_3OD of decomposition products of electrolyte solvents: HCOOLi, CH_3COOLi, 1,2-propanediol and triethylene glycol dimethyl ether; * -solvent residues.

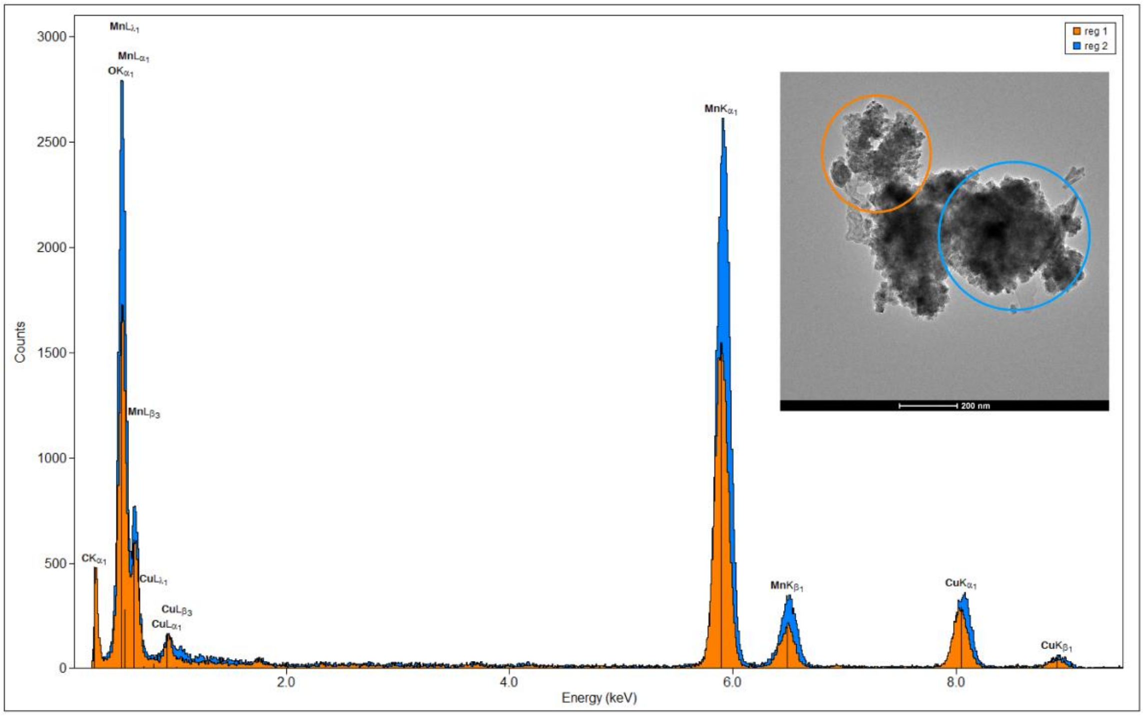

Figure S37. EDS analysis of the cathode material with different C: Mn: O content. The copper element comes from the use of copper-carbon grids.

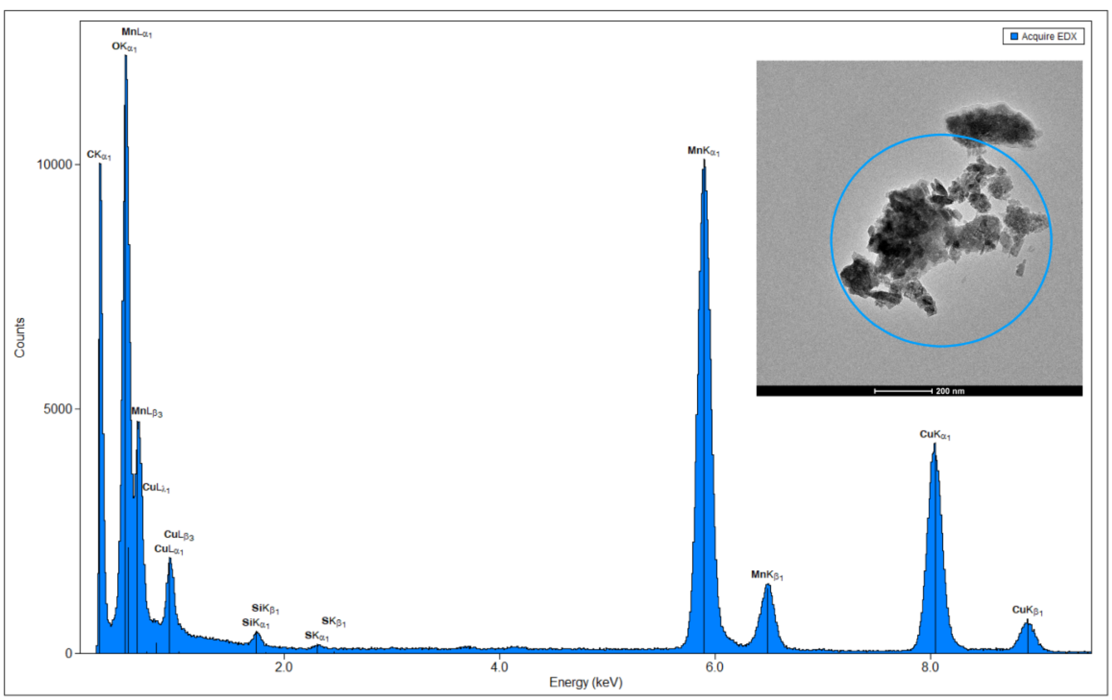

Figure S38. EDS analysis of the cathode material with different C: Mn: O content. The copper element comes from the use of copper-carbon grids.

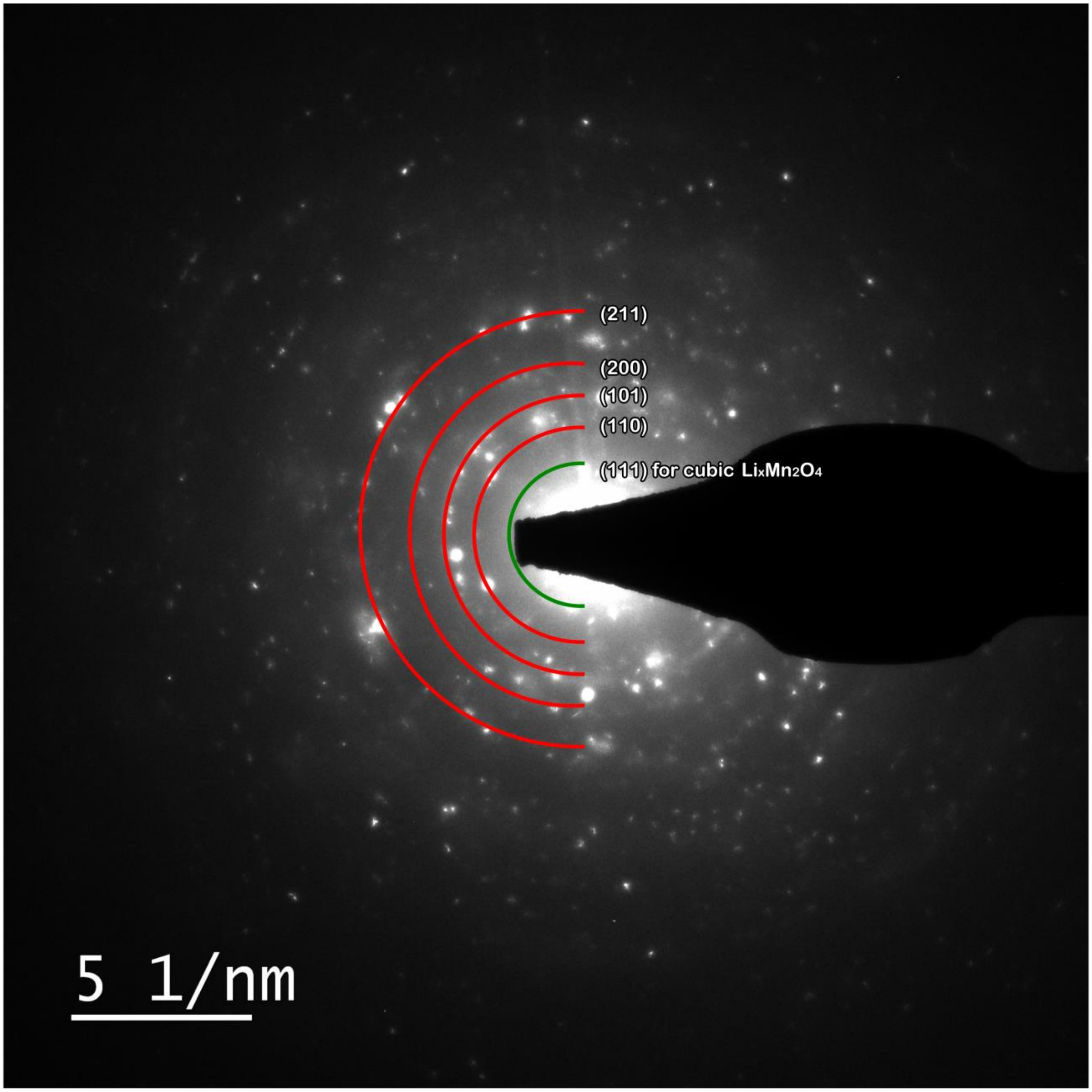

Figure S39. The selected area electron diffraction (SAED) pattern of cathode material, β-MnO_2 (red) and $Li_xMn_2O_4$ (green).

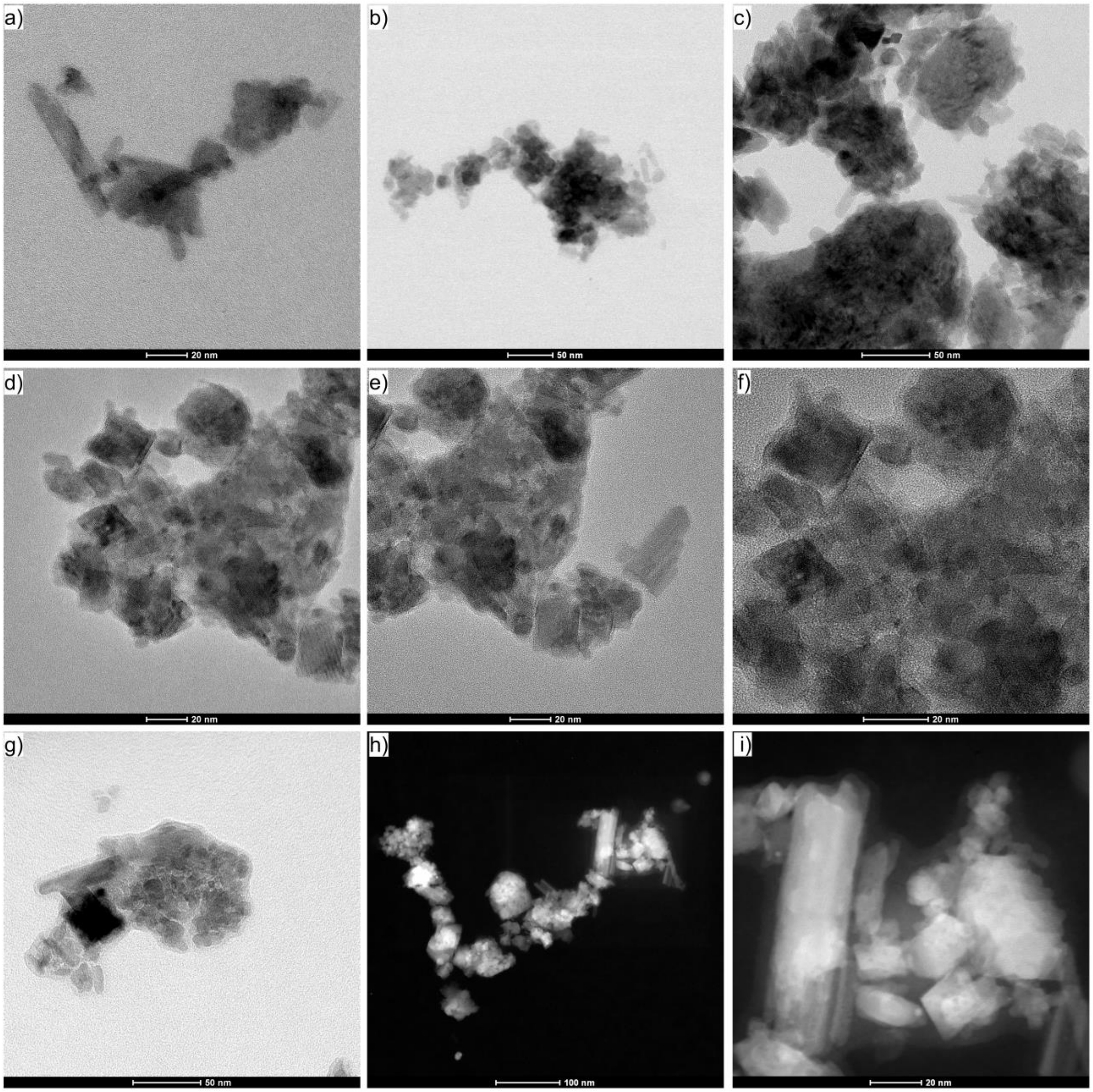

Figure S40. TEM micrographs of cathode material containing rod-shaped nanocrystals of β-MnO_2 (a-c), nanocrystals of $Li_xMn_2O_4$ (d-f), and a mixture of both (g-i).

[1] Petrus, R.; Fałat, P.; Sobota, P. Use of lithium aryloxides as promoters for preparation of α-hydroxy acid esters, *Dalton Trans.* **2020**, *49*, 866-876.